UNIVERSIDADE FEDERAL DO CEARÁ
FACULDADE DE MEDICINA
DEPARTAMENTO DE FISIOLOGIA E FARMACOLOGIA
PROGRAMA DE PÓS-GRADUAÇÃO EM FARMACOLOGIA

CLARA NORÕES NOGUEIRA

PI3Kγ INHIBITION INDUCES IMMUNOGENIC BIOMARKERS IN HEMATOLOGICAL CANCER CELLS *IN VITRO*

FORTALEZA - CE
2024
CLARA NORÕES NOGUEIRA

PI3Kγ INHIBITION INDUCES IMMUNOGENIC BIOMARKERS IN HEMATOLOGICAL CANCER CELLS *IN VITRO*

Dissertation presented to the Post-graduate in Pharmacology Program, of the Faculty of Medicine at the Federal University of Ceara, as a partial requisite to obtaining the title of Master in Pharmacology.
Advisor: Prof. Dr. Diego Veras Wilke
Co-advisor: Profa. Dra. Alessandra Ghigo

FORTALEZA - CE
2024

CLARA NORÕES NOGUEIRA

PI3Kγ INHIBITION INDUCES IMMUNOGENIC BIOMARKERS IN HEMATOLOGICAL CANCER CELLS *IN VITRO*

Dissertation presented to the Post-graduate in Pharmacology Program, of the Faculty of Medicine at the Federal University of Ceara, as a partial requisite to obtaining the title of Master in Pharmacology.

Approved in: 19/02/2024.

EXAMINERS

_____

Prof Dr. Diego Veras Wilke (UFC)

_____

Profa. Dra. Alessandra Ghigo (UNITO)

_____

Prof. Dr. Roberto César (UFC)

_____

Dra. Camila Fernandes (UFC)

Dados Internacionais de Catalogação na Publicação
Universidade Federal do Ceará
Sistema de Bibliotecas
Gerada automaticamente pelo módulo Catalog, mediante os dados fornecidos pelo(a) autor(a)

N711p Nogueira, Clara Norões.
PI3K gamma inhibition induces immunogenic biomarkers in hematological cancer cells in vitro / Clara Norões Nogueira. – 2024.
69 f. : il. color.

Dissertação (mestrado) – Universidade Federal do Ceará, Faculdade de Medicina, Programa de Pós-Graduação em Farmacologia, Fortaleza, 2024.
Orientação: Prof. Dr. Diego Veras Wilke.
Coorientação: Profa. Dra. Alessandra Ghigo.

1. leucemia mielóide crônica. 2. biomarcadores imunológicos. 3. morte celular imunogênica. I. Título.
CDD 615.1

ACKNOWLEDGEMENTS

I want to express my gratitude towards all of those who contributed directly and indirectly to the completion of this work. Firstly, I want to thank Prof. Dr. **Diego Veras Wilke** for accepting me into the laboratory, for the enthusiasm, hopefulness and for always inspiring me to persevere even when things didn't go as planned. My growth as a researcher is majorly due to the examples set by you. To Dr. **Thaís Brito**, my close friend and lab colleague, this work would not be complete without your help, advice, and interference. I admire you and your commitment to everything you aspire to, and desire nothing but success in this new phase in your career.

To my mother **Albaceli** and father **Ricardo** for the support, love and encouraging words. To my sister **Helena**, one of my biggest cheerleaders, thank you for believing in me and always showing enthusiasm with my research and academic ambitions. To my grandmothers **Alba** and **Maria Fiel** (*in memoriam*) that always supported my dreams and aspirations.

To **Biatriz**, my love, for the partnership we share, for being my anchor, my support, for always cheering for me and showing interest in my work. To **Lina**, my cat, who kept me company while I was writing. To **Raquel** and **Vinícius** for all the laughs and moments of joy. To **Mariana, Iara** and **Maria** for the years of friendship, advice and never-ending support. To **Joaquim, Jamille, Bruna, Luzia, Mayra** and **Claudia**, my friends from Fiocruz, for all the moments shared. To my great friends from Italian class, **Lorena**, **Edvan** and **Renatta** for all the companionship and for sharing the stress and anxiety before each test.

To my LaBBMar colleagues, **Alexia**, **Felipe**, **Keilla** for the exchange of knowledge, research and partnership. To my great friends and lab family **Katharine**, **Maísa**, **Yuri**, **Eduardo**, **Mariana** and **Andrea** for all the laughs, lunches, coffee time, advice, gossip and complicity. You all made this journey feel lighter and fun.

To Professor **Roberto César** and **Dra. Camila Fernandes** for accepting to contribute to this work. To Prof. Dr. **Alessandra Ghigo** for accepting to be my co advisor and providing valuable insights and support. I have great admiration for all your work, research and intelligence.

To Prof. Dr **João Agostinho** for receiving me so well at USP, being so patient and kind to teach and exchange your expertise. I also want to thank **Anali** for all the assistance with experiments and **Keli Lima**, **Bruna**, **Hugo**, **Jean** and **Natália** for always being willing to teach and help.

To the Coordenação de Aperfeiçoamento de Pessoal de Nível Superior (**CAPES**) for the scholarship awarded to me, to the **Unidade Multiusuário** from the Núcleo de Pesquisa e Desenvolvimento de Medicamentos for technical support. To **CNPq**, **CAPES** and **INCT** for the financial support which made this work possible.

ABSTRACT

PI3Kγ INHIBITION INDUCES IMMUNOGENIC BIOMARKERS IN HEMATOLOGICAL CANCER CELLS *IN VITRO*

Chronic myeloid leukemia (CML) is a subtype of hematological malignancy characterized by the presence of a chromosomal translocation which results in *Bcr/Abl1* gene fusion. Therapy with tyrosine kinase inhibitors revolutionized treatment of CML patients, however about 20-30% develop resistance. The phosphoinositide 3-kinases (PI3K) are a family of lipid kinases with roles in cell signaling, activation and metabolic regulation. The PI3K pathway is found deregulated in many human cancers. Class IB PI3Kγ is enriched in myeloid cells and has important roles in innate immunology as it regulates migration, differentiation, and activation of myeloid cells. Immunogenic cell death (ICD) is a type of regulated cell death which induces immunological response against dying cancer cells, constituting an interesting therapeutic strategy. The response is activated by damage-associated molecular patterns (DAMPS), namely calreticulin (CALR), high-mobility group box 1 protein (HMGB1), heat shock proteins (HSPs), among others. As PI3Kγ displays important roles in regulating immune response in myeloid cells, the development of PI3Kγ inhibitors could be an interesting immunogenic strategy. This work aimed to assess the capability of PI3Kγ inhibitors to elicit immunogenic cell death by evaluating the presence of some of the crucial DAMPs. Expression of PI3Kγ in several cell types was detected by flow cytometry. Inhibitors used were evaluated *in silico* for target and pharmacological parameters prediction. Reduction of cell viability was perceived in trypan dye exclusion assay for both molecules at 3000, 1000 and 300 nM. Colony formation assay showed reduction of the number of K562 colonies at the 2000 and 1000 nM concentration for AS-605240, and at 2000, 1000 and 300 nM for IPI-145. Both inhibitors caused morphologic alterations such as shrinkage and high granularity increase. Additionally, CALR externalization was detected, while AS-605240 and IPI-145 at 1000 nM increased nuclear HMGB1. In western blot, K562 cells treated with IPI-145 reduced p62 expression, suggesting autophagic flux induction. AS-605240 at 100 nM and IPI-145 at 100, 300 and 1000 nM were able to increase phosphorylation of eIF2α. Therefore, AS-605240 and IPI-145 showed antiproliferative effects, induced cell stress and activated markers of immunogenicity. Thus, the perspective of chemotherapy associated with PI3Kγ inhibitors to elicit or burst ICD is a promising strategy, however further studies are necessary.

Keywords: chronic myeloid leukemia, immunological biomarkers, immunogenic cell death.

RESUMO

INIBIÇÃO DE PI3Kγ INDUZ MARCADORES IMUNOGÊNICOS EM LINHAGENS DE TUMORES HEMATOLÓGICOS *IN VITRO*

Leucemia mieloide crônica (CML) é um subtipo de neoplasia hematológica caracterizada por uma translocação cromossômica que acarreta a fusão gênica *Abr/Bcl1*. A terapia com inibidores de tirosina cinase revolucionou o tratamento, mas cerca de 20 a 30% dos pacientes adquirem resistência. Fosfatidilinositol 3-cinases (PI3K) são uma família de cinases com papéis em sinalização celular, ativação e regulação metabólica. A via das PI3Ks é desregulada em diversos tipos de cânceres. PI3Kγ, único membro da classe IB, tem sua expressão enriquecida em células mieloides e a sua sinalização é crucial para a resposta de imunidade inata, já que regula migração, diferenciação e ativação de células mieloides. Morte celular imunogênica é um tipo de morte regulada que promove resposta imune contra as células em processo de morte. Essa resposta é ativada por padrões moleculares associados à dano (DAMPs) liberados no processo de morte celular, como a calreticulina (CALR) High-mobility group box 1 protein (HMGB1), proteínas de choque térmico (HSPs), entre outros. Como PI3Kγ possui funções importantes na regulação da resposta imune, a terapia com inibidores de PI3Kγ pode ativar marcadores imunogênicos. O presente trabalho objetivou avaliar a capacidade dos inibidores de PI3Kγ de induzir alguns marcadores relacionados a ICD. A expressão de PI3Kγ em várias linhagens celulares foi avaliada por citometria de fluxo. Os inibidores utilizados foram analisados *in silico* para predição de alvos. Atividade antiproliferativa dos inibidores de PI3Kγ, AS-605240 e IPI-145, foi observada nos ensaios de exclusão de azul de tripan em células K562 e formação de colônias em células K562 e Jurkat. A redução da viabilidade celular foi percebida para ambas as moléculas em concentrações entre 3000 nM a 300 nM. O ensaio de formação de colônias mostrou redução de colônias de K562 nas concentrações de 2000 e 1000 nM para AS-605240 e nas concentrações de 2.000, 1.000 e 300 nM para IPI-145. AS-605240 e IPI-145 causaram alterações morfológicas como redução do tamanho celular e aumento de granularidade. A externalização do CALR foi detectada, em conjunto com o aumento da fosforilação de eIF2α. Em western blot, nas células K562, o tratamento com IPI-145 reduziu a expressão de p62, sugerindo indução de fluxo autofágico. Portanto, AS-605240 e IPI-145 apresentam atividade antiproliferativa, causam estresse celular e induzem marcadores de imunogenicidade. Dessa forma, o tratamento quimioterápico associado com inibidores de PI3Kγ pode ser uma estratégia promissora, porém estudos adicionais são necessários.

Palavras-chave: leucemia mielóide crônica, biomarcadores imunológicos, morte celular imunogênica.

FIGURE LIST

TABLE LIST

ACRONYMS AND ABBREVIATIONS

ALL - Acute lymphoid leukemia

AML - Acute myeloid leukemia

ANOVA - Analysis of Variance

ATP - Adenosine triphosphate

$C0_2$ - Carbonic gas

DCs - Dendritic cells

CALR - Calreticulin

CLL - Chronic lymphoid leukemia

CML - Chronic myeloid leukemia

DAMPs - Damage associated molecular patterns

DAPI - 4,6-diamidino-2-phenylindole

DMEM - Dulbecco's Modified Eagle Medium

DMSO - Dimethyl Sulfoxide

DOX - Doxorubicin

FBS - Fetal bovine serum

FDA - Food and drug administration

FSC - Forward scatter

GCO - Global Cancer Observatory

GPCR - G-protein coupled receptors

HMGB1 - High mobility group box protein 1

HSP - Heat shock proteins

ICD - Immunogenic cell death

IFN-1 - Interferons type I

INF-α - Interferon alpha

IFN-γ - Interferon gamma

IL-12 - Interleukin 12

IMDM - Iscove Modified Dulbecco Media

INCA - National Cancer Association

IPGS - inactivated PI3Kγ syndrome

KO - Knockout

MAPK - Mitogen-activated protein kinase

MHC - Major histocompatibility complex

mTORC1 - Mammalian (or mechanistic) target of rapamycin complex 1

nM - Nanomolar

PBS - Phosphate buffered saline

PDK1 - Phosphoinositide-dependent protein kinase-1

PE - Phycoerythrin

p-eIF2α - Phosphorylated eIF2α

Ph - Philadelphia chromosome

PI3K - Phosphoinositide 3-kinases

PIP3 - PtdIns-3,4,5-P3

PtdIns - Phosphatidylinositols

PTEN - Phosphatase and tensin homolog deleted on Chromosome 10

p-S6RP - Phosphorylated S6RP

Tdp1 - Tyrosyl-DNA Phosphodiesterase

TK - Tyrosine kinase

TKI - Tyrosine kinase inhibitor

TRL - Toll-like receptors

RPMI - Roswell Park Memorial Institute

SLL - Small lymphocytic lymphoma

SSC - Side Scatter

USP - Universidade de São Paulo

Vps34 - Vacuolar protein sorting 34

WHO - World Health Organization

µL - Microliter

µM - Micromolar

SUMMARY

1. INTRODUCTION

1.1 Cancer

Cancer is the name given to an extensive number of diseases which could initiate in any body tissue or organ. It is characterized by an abnormal cell growth and subsequent invasion of adjoining parts of the body or other organs. Cancer is the second leading cause of death globally, being responsible for one in six deaths in 2020 (World Health Organization, WHO). The three more prominent cancer types in 2020, regardless of gender were: breast, lung and colorectal cancer. Those responsible for the most deaths were lung, colorectal and liver cancer, respectively (WHO - International Agency for Research on Cancer, 2020).

According to the Global Cancer Observatory (GCO), in 2040 the estimated number of new cases will be 30.2 million and the number of associated deaths will be around 16.3 million (GCO, 2020). In Brazil, the National Cancer Institute (INCA) estimates there will be 704 thousand new cases per year till 2025, counting the three-year period 2023-2025. The most common malignancy in Brazil is the non-melanoma skin cancer, followed by breast, prostate, colorectal, lung and stomach (INCA, 2023). Hematological cancers are also among the ten most common malignancies in Brazil, with non-Hodgkin's lymphoma incidence being relevant in men and women, while leukemias represent 2.8% of all women's cancer deaths (INCA, 2023).

The carcinogenesis of solid or hematological tumors occurs usually over extended periods of time and is common for it to take years before detection. This process is typically described for solid tumors and it is divided into three main stages: initiation, promotion, and progression. In the initiation stage, the genes are affected by the carcinogenic agent, suffering modifications, even though it is not clinically possible to detect a tumor. The progression stage is characterized by the initiated cells being affected by carcinogens.

Cancer cells share characteristics acquired in the process from normal cells to malignant tumors. These are referred to as The Hallmarks of Cancer, proposed by Hanahan and Weinberg in 2000, with new additions being proposed in 2011 and 2022. The hallmarks are a concept which allows the understanding that even though different cancer types have diverse capabilities and characteristics, some are shared across the spectrum of human cancer. The hallmarks currently are the capacity to sustain proliferative signaling, evading growth suppressors, avoiding destruction by immune cells, enabling replicative immortality, tumor-

promoting inflammation, activating invasion and metastasis, inducing, or accessing vasculature, genome instability and mutation, resisting cell death and deregulating cellular metabolism. The last emerging hallmarks were deregulating cellular metabolism and avoiding immune destruction which are now included as core characteristics. The inclusion of enabling characteristics is justified by the need to include capabilities addressing the cancer pathogenesis and the mechanisms developed by preneoplastic cells to acquire the phenotypes for tumor malignancy. The proposed enabling characteristics are non-mutational epigenetic reprogramming and polymorphic microbiomes. The first refers to the fact that genome reprogramming occurs without mutations, which can happen epigenetically for several reasons, one of them being alterations in the environment. The latter refers to how microbiomes affect health and disease, as it is present in many barrier tissues of the body exposed to external environments such as the gastrointestinal tract, lungs, and urogenital system. It has been found there are polymorphic variations in individual microbiomes and mostly bacteria can have protective or detrimental effects on carcinogenesis, malignant progression, and therapy efficacy. Currently, the emerging hallmarks are unlocking phenotypic plasticity and senescent cells. Phenotypic plasticity is the capability to evade cell differentiation, a process which is not advantageous to neoplastic cells as it constitutes a barrier to proliferation. Cellular senescence is a form of seizing cellular proliferation, probably to keep homeostasis. This process occurs mostly as a support for programmed cell death mechanisms to remove diseased or dysfunctional cells and was viewed as a protective mechanism against cancers. Opposing that idea, many reports have shown in some contexts senescence is a positive stimulus for cancer progression through the activation of a senescence-associated secretory phenotype which can trigger signaling molecules that can confer hallmark capabilities to neighboring cells (Hanahan, 2022). Ultimately, it is noticeable cancer cells have a complex subset of interactions, with a multifactorial process of tumor formation and progression dependent of genetic/epigenetic changes and the microenvironment (Baghban *et al*., 2020), evidence which allows the comprehension of cancer as a nuanced subset of diseases with challenging therapies.

Figure 1 - The Hallmarks of Cancer.

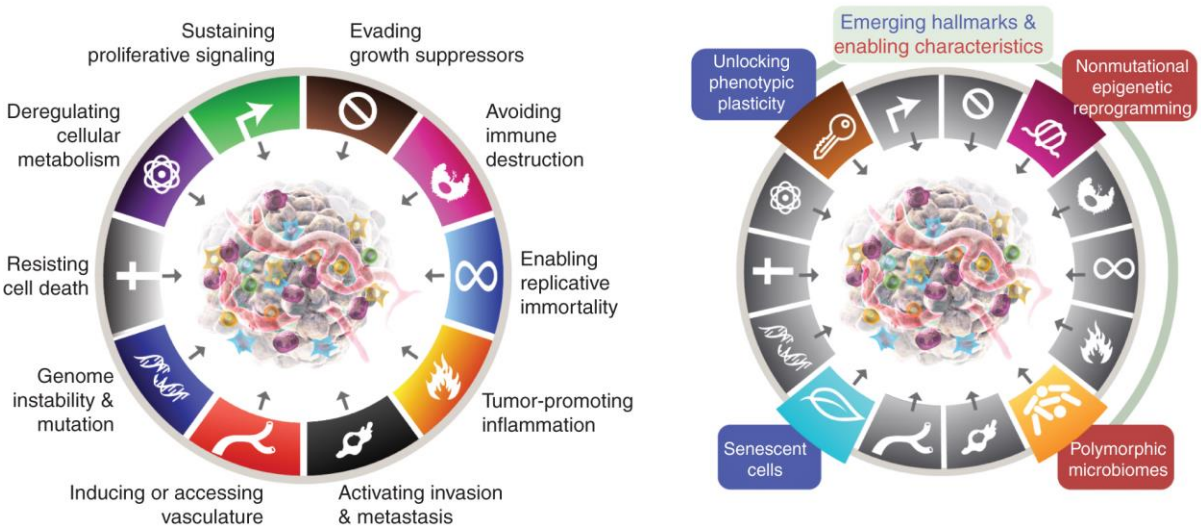

Source: HANAHAN, 2022.

The left scheme depicts the current hallmarks (2022) which are sustaining proliferative signaling, evading growth suppressors, avoiding immune destruction, enabling replicative immortality, tumor-promoting inflammation, activating invasion and metastasis, inducing or accessing vasculature, genome instability and mutation, resisting cell death, deregulating cellular metabolism. The right figure shows the emerging hallmarks and enabling characteristics proposed by Hanahan (2022): unlocking phenotypic plasticity and senescent cells, non-mutational epigenetic reprogramming, polymorphic microbiomes.

Hematological cancers or malignancies are the current nomenclature to define a collection of diverse conditions originating from bone marrow cells and the lymphatic system (Rodriguez-Abreu; Bordoni; Zucca, 2007). These types of disorders are accountable for about 6.5% of all cancers worldwide (De Moraes Hungria *et al*., 2019) and they are divided into three major types: leukemia, lymphoma and multiple myeloma. Incidence varies based on subtype of cancer, gender, age and socioeconomic factors (Keykhaei *et al*., 2021). However, it has been shown the occurrence of leukemia has only increased for people aged over 70 (Zhou et al., 2019). The rate of hematological cancers has been rising since 1990, which has been accompanied by an aging population, provoking a challenge to health care systems (Zhang *et al*., 2023). Hematological malignancies are classified in several types, with the most common being leukemia, multiple myeloma, non-Hodgkin lymphoma, and Hodgkin lymphoma (Damlaj; El Fakih; Hashmi, 2019). The spectrum of subtypes rates globally is ever changing, with leukemias declining worldwide but rising in some developed regions such as France, Spain, Slovenia, and Cyprus (Zhang *et al*., 2023). These cancers are an important cause of death globally, with 1.3 million new cases reported in 2020 and 700,000 deaths (Chen *et al*., 2022).

Lymphomas account for about half of the blood cancers and constitute a heterogeneous group of neoplasms originating typically from lymphoid organs and are derived from lymphocytes. There are currently over ninety subtypes, with very diverse epidemiology, pathology, clinical presentation and response to treatment (Lewis; Lilly; Jones, 2020).

Leukemias are cancers of the body's blood forming tissues, including the bone marrow and the lymphatic tissue. They are characterized by the clonal expansion of leukemic cells in the bone marrow, increasing the number of the affected lineage cells in circulation (Baeker Bispo; Pinheiro; Kobetz, 2020). Principal types of leukemia include acute lymphocytic (lymphoid) leukemia (ALL), acute myelogenous (myeloid) leukemia (AML), chronic lymphocytic leukemia (CLL) and chronic myelogenous leukemia (CML) (Mayo Clinic, 2022). Myeloid leukemias initiate in early myeloid cells, progenitors of leucocytes, platelets, or megakaryocytes. Lymphocytic leukemias occur in the progenitors of lymphocytes (American Cancer Society, 2018).

1.1.1 *Chronic myeloid leukemia*

CML is a clonal expansion of primitive progenitor myeloid cells, and it was the first human disease in which a link with altered karyotype could be linked to pathogenesis (Faderl *et al*., 1999). Patients with CML have a chromosomal alteration called the Philadelphia chromosome (Ph), which is the product of a reciprocal translocation between chromosomes 9 and 22. The Ph is a hallmark of CML and is found in 95% of patients. This fusion results in a new hybrid gene called Bcr-Abl (Breakpoint cluster region-Abelson murine leukemia) is created and is transcribed as a chimeric messenger RNA (Faderl *et al*., 1999). The ABL1 gene encodes a non-receptor tyrosine kinase (TK) with important roles in cell signaling and growth regulation (Faderl *et al*., 1999). Normal Abl protein functions include regulation of cell cycle, cellular response of genotoxic stress and integrin signaling (Deininger *et al*., 2000). The product of the BCR-ABL1 fusion is an oncoprotein with TK activity stimulating hematopoietic transformation and myeloproliferation (Pophali; Patnaik, 2016). This aberrant TK has upregulated activity and causes downstream activation of several metabolic and signaling pathways, like for instance JAK/STAT, PI3K/AKT, RAS/MEK, mTOR, Src kinases (Pophali; Patnaik, 2016).

Dissimilar to AML, the chronic presentation of the disease takes longer to develop. CML is usually divided into three stages, the chronic phase, accelerated phase, and blast phase. Most patients are diagnosed in the chronic phase, with little to no symptoms. The diagnosis is

based on abnormal blood cell count, with most patients being in this phase for a few years. Without treatment, CML usually progresses to the subsequent phases. In the accelerated phase there are some symptoms associated with enlarged spleen, low red blood cell counts and abnormal count of white blood cells. The blast phase is characterized by presence of 20% or more neoplastic cells in peripheral blood or marrow or the presence of extramedullary blast cells. The symptoms become more severe, and shortness of breath, infections and bleeding can occur. At this stage it can rapidly develop into AML or ALL (Abramson Cancer Center, Penn Medicine). In one third of cases the blasts have a lymphoid morphology and markers, such as CD10. Blast phase is usually lethal in months, as it progresses rapidly.

Initially, treatment was focused on Interferon alpha (INF-α) and allogeneic stem cell transplantation. INF-α produced improvement on overall survival, however was related to poor tolerability and progression of the disease. Although allogeneic stem cell transplantation is considered curative, it has high morbidity and mortality, which reduces its application (Pophali; Patnaik, 2016).

The development of tyrosine kinase inhibitors (TKI) revolutionized treatment, and most patients don't progress to the blast phase. Ten year overall-survival is 80-90%. Due to TKI treatment, the accelerated phase is rarely seen, being omitted from several sources (Pérez-Jiménez; Derényi; Szöllősi, 2023). The first of these molecules reported was imatinib mesylate, who showed better survival rates when compared with INF-α and cytarabine therapy, also being more tolerated. Despite its advantages, over time 20-30% of patients developed TKI resistance to imatinib, which was accredited to mutations on the BCR-ABL1 TK. Additionally, other inhibitors emerged such as nilotinib, dasatinib, bosutinib and ponatinib. These have the capability to inhibit more TK proteins, and not only the BCR-ABL1 (Pophali; Patnaik, 2016). Even though new strategies were used to develop new TKI, resistance is still an issue. The T315I mutation, for instance, causes resistance in about 20% of cases for all inhibitors except Ponatinib. Consequently, other therapeutic targets are being evaluated in the pathways downstream of TK activation, such as the PI3K/Akt/mTOR pathway (Singh *et al*., 2021).

1.2 PI3K Pathway

The phosphoinositide 3-kinases (PI3K) are a group of conserved lipid kinases with important signaling, activation and regulation of metabolism roles. They are a family of heterodimeric enzymes formed by a catalytic (p110) and adaptor or regulatory subunit. There are four isoforms of the catalytic unit (α, β, γ, and δ) and multiple regulatory subunits (p85α,

p85β, p50α, p55α and p55γ). Each isoform characterizes one of the class I enzymes (Noorolyai *et al*., 2019).

In general, PI3Ks promote the phosphorylation of the 3'-OH group of phosphatidylinositols (PtdIns) on the plasma membrane (Martini *et al*, 2014). PI3Ks and its signaling pathways have been established as key players in multiple cellular processes such as metabolism, inflammation, cell survival, motility, and cancer progression (Martini *et al*, 2014). Class I PI3Ks are divided in class IA, composed of PI3Kα, PI3Kβ, and PI3Kδ, and class IB represented by PI3Kγ. Activation of the pathway occurs through receptor tyrosine kinase (RTK) or G-protein coupled receptors (GPCRs) which recruits the PI3Ks to the plasma membrane. Class IB is activated exclusively by Gβγ subunits downstream of GPCRs, although it has been shown that class IA PI3Kβ can also be activated by GPCRs through the same subunit (de Santis *et al*., 2019).

Figure 2 - Illustration of the PI3K signaling pathway and its downstream targets.

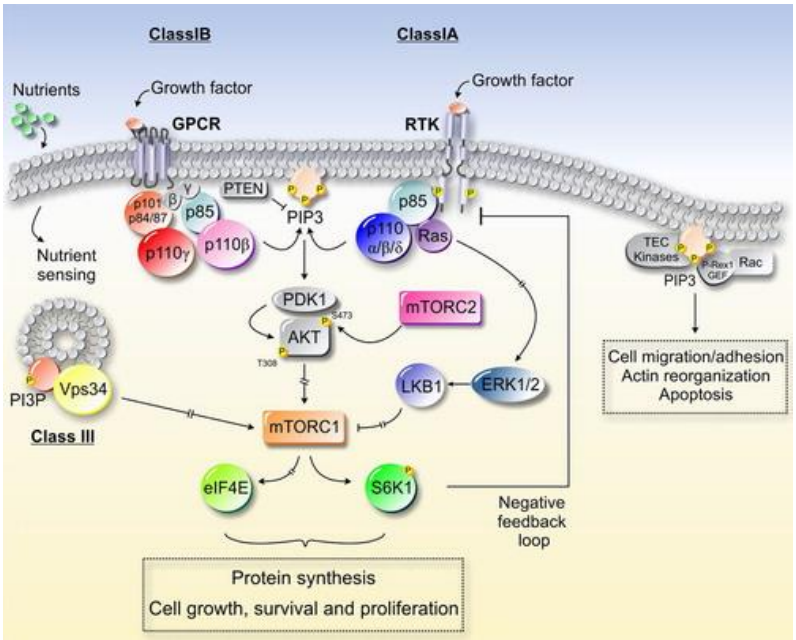

Source: Martini *et* al, 2014.
Class I PI3Ks are commonly activated by growth factors and mediate catalysis of second messenger PIP3. PIP3 then activates other signaling pathways, namely AKT. Class III PI3Ks are activated by nutrients in a nutrient sensing manner.

Class II PI3Ks have three different isoforms PI3K-C2α, PI3K-C2β (broadly expressed) and PI3K-C2γ. Differently from Class I PI3Ks they possess additional protein-binding domains and extended N-Terminal region which contributes to intracellular localization. *In vitro* they

have not produced PIP3, however are able to produce PIP2 from PI. Class III PI3K is composed of vacuolar protein sorting 34 (Vps34), being the ancestral member of the PI3K family and present in all eukaryotes. Vps34 promotes conversion of PI in PI(3)P, a secondary messenger involved in important lysosomal pathways such as autophagy and phagocytosis (de Santis *et al*., 2019).

Usually, the p110 catalytic subunit of PI3K enzymes is stabilized by dimerization with the corresponding regulatory subunit. The pathway is activated by several extracellular stimuli like growth factors, cytokines, and hormones (Yang *et al*., 2019). The enzyme catalyzes the phosphorylation of PtdIns-4,5-P2 to generate PtdIns-3,4,5-P3 (PIP3), which acts as a second messenger recruiting proteins from the cytoplasm. In normal physiological conditions PIP3 is quickly metabolized by lipid phosphatases like the tumor suppressor tumor suppressor phosphatase and tensin homolog deleted on Chromosome 10 (PTEN) which terminates signaling via the removal of the 3'-phosphate. PTEN is essential for regulating the PI3K signal transduction. In many cancers there's loss of PTEN function, elevating basal and stimulated levels of PIP3 by reducing the inactivation of the second messenger. In that manner, loss of the regulating function is frequently exploited for the survival and growth of cancerous cells.

Downstream of the second messenger is the Akt-mTOR signal transduction pathway, with Akt being recruited alongside with phosphoinositide-dependent protein kinase-1 (PDK1). PDK1 is responsible for phosphorylating Akt, which can activate various effector targets such as the mammalian (or mechanistic) target of rapamycin complex 1 (mTORC1), controlling several cellular survival processes (Papa; Pandolfi, 2019). Akt controls mTORC1's function through molecular mechanisms, namely the tumor suppressive tuberous sclerosis complex which is phosphorylated upon Akt being stimulated which allows activation of mTORC1 on lysosomes. After activation of mTORC1, it engages with the Ragulator complex and if there are nutrients, activates anabolic processes, namely lipids and nucleotide synthesis, cell growth and proliferation (Papa; Pandolfi, 2019).

As mentioned previously, abnormal PI3K signaling is correlated to many human cancers. Mutations of the enzyme or inactivation of negative regulator PTEN are among the common factors for carcinogenesis. Genetic variations have been detected in all levels of the PI3K/Akt cascade, with PI3Kα (PIK3CA) being referred to as an oncogene playing significant roles in ovarian (Shayesteh *et al*., 1999), colorectal, glioblastoma, gastric, breast, lung and kidney cancers (Samuels; Waldman, 2010).

Over-activation of this pathway acts on its downstream targets contributing to proliferation, invasion and metastasis. Since the PI3K/Akt/mTOR is one of the most important

signal transduction pathways, the abnormal activation has been correlated to several types of cancers (Rascio *et al*., 2021). Thus, there are massive efforts to find drugs able to target signaling via this pathway. Additionally, oncogenic variations of PI3K signaling are correlated to resistance to specific antineoplastic therapies.

1.2.1 *PI3Kγ*

PI3Kγ is the sole member of the class IB, is primordially activated by G-protein-coupled receptors (G-PCR) and RAS family GTPases (Lanahan; Wymann; Lucas, 2022) (Zhu *et* al, 2019), playing significant roles in cell signaling. Aside from the canonic mechanisms of activation it has been shown that it can be activated downstream of the high affinity IgE receptor (FcεRI) (Lanahan; Wymann; Lucas, 2022). The activation of the class IB enzyme has been shown to regulate mitogen-activated protein kinase (MAPK) cascades, being able to trigger more than one signaling pathway downstream of GPCRs (Rückle; Schwarz; Rommel, 2006). This signaling has a similar basis in any type of stimuli which can have different outputs depending on the cell metabolism and epigenetic profile. Buildup of the second messenger, PIP_3, leads to the recruitment of proteins with pleckstrin homology (PH) domains, like AKT (Lanahan; Wymann; Lucas, 2022).

Differently from the other classes of PI3K, the gamma type expression was considered to be restricted to hematopoietic cells of myeloid origin (Lanahan; Wymann; Lucas, 2022) initially. However, some recent studies have demonstrated its expression is indeed widely distributed (Nürnberg; Beer-Hammer, 2019). There are reports of PI3Kγ distribution in endothelial cells, microglia, tubular cells of the kidney and prostate gland cells, nevertheless these data have to be taken with caution due to possible contamination from blood cells (Nürnberg; Beer-Hammer, 2019). PI3Kγ also plays a crucial role in response against infections by driving IFN production, and recruiting NK and CD8+ T cells (Sala *et al*., 2021). Furthermore, PI3Kγ activity is required for T-cell activation and differentiation, as well as for an efficient T-cell mediated immune response (Ladygina *et al.*, 2013). Additionally, PI3Kγ is found deregulated in solid tumors, such as gastrointestinal cancers (Falasca; Maffucci, 2014). However, expression is constitutively enriched in leukocytes (Sala *et al*., 2021). The PI3Kγ signaling cascade is crucial to the normal functioning of myeloid cells, as it regulates migration, differentiation, and activation of myeloid-derived immune cells (Gu *et al*., 2023). Beside the catalytic function, the enzyme also possesses a scaffold function, acting as an A-Kinase

anchoring protein (Sala *et al*., 2021). Since PI3Kγ is at the center of multiple signaling cascades, it constitutes an important pathway that needs to be elucidated and comprehended.

PI3Kγ can also be activated by pathogen and damage-associated molecular patterns downstream of Toll-like receptors (TRL), regulating metabolic and immune homeostasis (Sala *et al*., 2021). Derivations in PI3Kγ regulation impacts several cell types, as the signal cascade is important to a healthy immune response. PI3Kγ-deficient mice have shown immune cell defects when exposed to pathogens, namely defective neutrophils migration and defects in the production of Reactive Oxygen Species (Lanahan; Wymann; Lucas, 2022). In mast cells, PI3Kγ deficiency have impaired autocrine GPCR signaling to augment degranulation and mediate edema. Comparably with neutrophils, macrophages and dendritic cells also show migration defects (Lanahan; Wymann; Lucas, 2022). It has also been related that PI3Kγ regulates the trafficking of inflammatory cells and the extent of cytokine response, having an important part to play in innate response, being referred as an innate checkpoint.

With the advance of genome studies, the PI3Kγ deficiency in humans was detected and characterized as inactivated PI3Kγ syndrome (IPGS), with two reported patients so far. In these cases, whole exome sequencing showed heterozygous alterations of *PIK3CG* encoding p110γ, the catalytic subunit of the enzyme. This loss-of-function variation was deemed as probably pathogenic. One of the patients displayed symptoms of hypotonia and prolonged fever, with laboratory results indicating mild thrombocytopenia, hypertriglyceridemia, increased lactate dehydrogenase and elevated ferritin (Thian *et al*., 2020). The second patient reported more severe symptoms, including antibody defects, associated cytopenias and infections, splenomegaly, and infiltration of T-cells in barrier tissues (Takeda *et al*., 2019). In that manner, is possible PI3Kγ deficiency could be correlated to abnormalities in innate cell morphology and function, with patients showing nontypical immune response and function (Thian *et al*., 2020). Experiments in PI3Kγ knockout (KO) mice showed traits similar to patients with IPGS. These findings demonstrate the potential of PI3Kγ as a target in diseases with inflammatory origins, such as asthma, cancer, idiopathic pulmonary fibrosis, cystic fibrosis, obesity, and many others.

Furthermore, PI3Kγ is responsible for promoting atherosclerotic lesions due to its role in chemokine-induced migration of monocytes/macrophages (Lanahan; Wymann; Lucas, 2022). Thusly, altered regulations of PI3Kγ in immunological cells are implicated in several disease processes.

PI3Kγ constitutes an interesting target to attenuate diseases with an immunology background due to its relatively selective expression and signaling redundancy, which could

reduce off-target toxicity and diminish adverse side effects of a possible pharmacological inhibitor.

1.3 PI3K inhibitors

PI3K inhibitors have shown interesting anticancer efficacy in many tumor subtypes, with copanlisib, alpelisib, idelalisib, duvelisib and umbralisib being approved by the Food and Drug Administration (FDA) and several new molecules are undergoing clinical trials. Adverse side effects of these inhibitors include hyperglycaemia, rash, diarrhea/colitis, hepatotoxicity, and hypertension and constitute major hurdles for the development and approval of new therapies (Yu *et al*., 2023). These PI3K inhibitors have varying range of selectivity, from Pan-inhibitors, Dual-inhibitors and Isoform-specific.

Pan-inhibitors can target the four isoforms of class I PI3K and are associated with a higher incidence of metabolic-related adverse events. Copanlisib (Aliqopa™; BAY 80–6946; Bayer AG) is a pan-class with potent activity for all four class I isoforms administered intravenously. It was approved by the FDA in 2017 for treatment of relapsed follicular lymphoma in adult patients who have received at least two prior systemic treatments (Yu *et al*., 2023). It shows efficacy as a monotherapy or as a combination treatment with other drugs. More common side effects include hyperglycemia, diarrhea, fatigue, and hypertension, which are mostly manageable (Dreyling *et al*., 2017). Copanlisib shows low toxicity when compared to other PI3K inhibitors, which can be attributed to its form of administration or intermittent dosage intervals (Yu *et al*., 2023).

An example of isoform-specific inhibitor is the small molecule Alpelisib (Piqray™; BYL719; Novartis), an oral selective inhibitor of PI3Kα which was approved by the FDA in 2019 in combination with fulvestrant for the treatment of postmenopausal women or men with HR-positive, HER2-negative, PIK3CA-mutated, advanced, or metastatic breast cancer. Although progression-free survival rates increased with treatment (André *et al*., 2019), in a first-in-human study of alpelisib in solid tumors 13,4% of participants discontinued treatment due to adverse effects. Hyperglycemia, rash, and diarrhea occur frequently and could be alleviated with treatment (Yu *et al*., 2023).

Idelalisib is an oral selective inhibitor with specificity for p110δ, the catalytic subunit of P3Kδ, was approved by the FDA in 2014 in association with rituximab for relapsed CLL. It has also been approved for relapsed follicular B cell non-Hodgkin lymphoma and relapsed small lymphocytic lymphoma (SLL) patients who have received at least two prior systemic

treatments. The drug carries a black box warning since there were reports of fatal and serious toxicity related to idelalisib (Yu *et al*., 2023). Hepatic toxicity, severe diarrhea, colitis, pneumonitis, infections, and intestinal perforation were some of the most severe side effects. Phase 1b and 2 studies showed most common side effects were fatigue, diarrhea, nausea, rash, chills, and pyrexia. One of the possible explanations for idelalisib associated toxicity is PI3Kδ inhibition of Treg cells can cause aberrations in T-cells, leading to cytotoxic T-cell organ infiltration (Cheah; Fowler, 2016). Considering idelalisib's toxicity, the FDA has removed accelerated approval for follicular lymphoma and elapsed SLL in 2022.

Duvelisib (Copiktra™; IPI-145; Verastem) is an inhibitor of isoforms PI3Kδ and PI3Kγ, with enhanced selectivity of 10-fold for the delta isoform. The selectivity for one isoform in detriment of the other can be credited to the conformation at the active site which opens a hydrophobic pocket not present in the apoenzyme. The compound binds at the ATP-binding region, a conserved site through the PI3K family. It also possesses a long target residence time, which can be correlated with improved duration of effect (Tangudu *et al*., 2019). Duvelisib received FDA approval in 2018 for treatment of CLL and SLL and was on the fast track for relapsed or refractory FL (Tangudu *et al*., 2019) however, the accelerated approval was removed by the FDA as a consequence of severe adverse effects. The drug carries a black box warning for the risk of fatal or severe infections, diarrhea/colitis, cutaneous reactions, and pneumonitis (Yu *et al*., 2023).

Umbralisib (UKONIQ™; TGR-1202; TG Therapeutics) is a dual inhibitor of PI3Kδ and casein kinase 1 epsilon with fast-track FDA approval in 2021 for adult patients with relapsed or refractory marginal zone lymphoma who have received at least one anti-CD20 based treatment. It is also on the accelerated approval for refractory FL with at least three prior systemic treatments (Yu *et al*., 2023). In clinical trials, umbralisib has reached satisfactory results with low incidence of adverse side effects. Most common Grade 3 or higher effects are neutropenia, diarrhea, and increased aminotransferase levels. The accelerated approval was removed by the FDA in 2022 since there is an increased risk of death for patients (Yu *et al*., 2023).

In april of 2022 the FDA published a briefing document regarding PI3K inhibitors for hematological malignancies delineating the most critical issues in developing these types of molecules, highlighting concerning trends in overall survival in multiple randomized controlled trials, toxicities of the PI3K inhibitor class, inadequate dose optimization, and trial design considerations regarding the limitations of single-arm trials. The selective PI3Kα inhibitor alpelisib was excluded from the discussion (FDA, 2022). These concerns may reflect future

clinical trials for PI3K inhibitors, with concerns being raised if single-arm-clinical trials are appropriate for approval of these molecules.

The only selective PI3Kγ inhibitor in clinical trials currently is Eganelesib or IPI-549 (Infinity Pharmaceuticals) (Yu *et al*., 2023). In preclinical studies, eganelesib was able to reprogram macrophages from the M2 phenotype to the M1 immune activated phenotype. The shift to the proinflammatory phenotype was able to magnify cytotoxic T cell activation at the tumor site. Association with nivolumab (anti-PD-1) demonstrated clinical activity, immune modulation, and favorable tolerability in a phase I clinical trial (De Vera *et al*., 2019).

AS-605240 is a specific inhibitor of PI3Kγ designed to be orally active and ATP-competitive. Studies have shown AS-605240 has attenuated joint inflammation progression in rheumatoid arthritis in mouse models, as well as regulation of autoimmune diabetes and autoimmune myocarditis. It has also evolved as a treatment or prevention of neurodegenerative diseases correlated with inflammation, being capable of ameliorating the streptozotocin-induced Alzheimer's disease in rats (Alluri *et al*., 2020). Association of AS-605240 with paclitaxel showed anticancer effects in Claudin-low triple negative breast cancer (Chang *et al*., 2020), being able to manipulate autophagy.

1.4 Immunogenic cell death

Anticancer therapies are usually classified between passive and active, depending on their ability to elicit immune response against malignant cells. Most chemotherapeutic agents are cytotoxic to cells in a tolerogenic or immune neutral manner (Bezu *et al*., 2018). Active therapies such as anticancer vaccines and checkpoint inhibitors have the capacity to engage the host's immune system, being advantageous therapies (Galluzzi *et al*., 2014).

Immunogenic cell death (ICD) is a type of cell death in which dying, stressed or injured cells can actively regulate immune response by exposing or releasing molecules (Kroemer *et al.*, 2022) to stimulate the immune system (Ahmed; Tait, 2020). These molecules are referred to as Damage-associated molecular patterns (DAMPs), which function as adjuvant or danger signals for the immune system. Some chemotherapeutic drugs, oncolytic viruses, physicochemical therapies and even radiotherapy can elicit ICD, if the host is immunocompetent (Ahmed; Tait, 2020). These DAMPs are recognized by innate pattern recognition receptors (PRRs) such as TLRs and NOD-like receptors, and as the cancerous cells are dying, promotes activation of tumor-specific immune responses. In view of this response, when an anticancer drug is capable of inducing ICD, there is a long-term efficacy correlated to

the toxicity to the cancer cells and to the antitumor immunity (Ahmed; Tait, 2020). For such an effect, there is evidence to corroborate treatment-driven ICD can reinforce the therapeutic actions of conventional anticancer chemotherapy and radiotherapy (Fucikova *et al*., 2020).

ICD is an emerging concept which was noted in cells treated with anthracyclines (such as doxorubicin, daunorubicin), oxaliplatin, bortezomib and some forms of radiotherapy, beyond the cytotoxicity effects can induce antitumor immunity, which enhances therapeutic efficiency (Krysko *et al*., 2012). For ICD to be induced, the dying tumor cells must release or expose certain DAMPs in a timely and ordained manner, which requires the cells to suffer enough stress (GARG *et al*., 2015). The cell surface exposure of 'eat me' signals like calreticulin (CALR), extracellular release of adenosine triphosphate (ATP) and liberation of high-mobility box group 1 (HMGB1) are some of the DAMPs involved in ICD (Ahmed; Tait, 2020), and can provide an indication if the phenomenon is induced or not. Other molecules of importance are heat shock proteins (HSP), type 1 interferons (IFN) and the phosphorylation of eIF2α, which is a pathognomonic factor for ICD (Bezu *et al*., 2018).

Figure 3 - Characteristics of Immunogenic Cell Death.

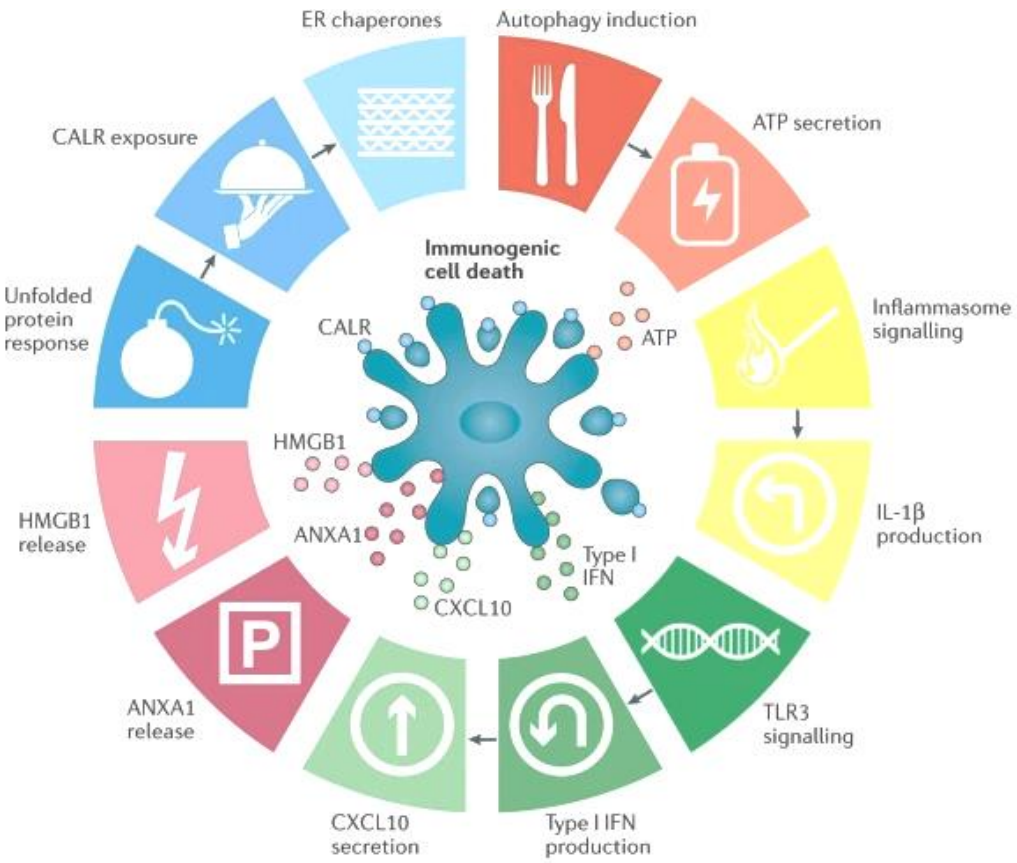

Source: Adapted from Galluzzi *et al*, 2016.

Processes required for ICD, like the unfolded protein response and subsequent CALR exposure and other endoplasmic reticulum (ER) chaperones on the cell surface, activation of autophagy and ATP secretion, liberation of interleukin-1β correlated to inflammasome signaling, activation of TLR3 which results in IFN response that stimulates production of ligand 10 of CXC-chemokine in addition to liberation of HMGB1 and annexin A1 (ANXA1).

CALR is exposed on the plasma membrane in response to ER stress and acts as an 'eat me' signal for dendritic cells (DCs) to phagocyte dying or dead cells. The exposure occurs due to molecular mechanisms including the phosphorylation of eIF2α, arrest of protein translation, activation of pro-apoptotic caspase 8, accompanied by cleavage of B-cell receptor-associated protein 31, aggregation of pro-apoptotic Bcl-2 family members at the outer mitochondrial membrane and proteins associated to vesicle transport to the Golgi apparatus and exocytosis (Fucikova *et al.*, 2020). Exposed CALR binds to CD91 (or LRP1), a chaperone sensing PRR expressed by antigen-presenting cells such as DCs.

Another relevant DAMP involved in ICD is HMGB1, a nuclear protein which when liberated extracellularly acts as a pro-inflammatory inducer (Ahmed; Tait, 2020). The release involves permeabilization of the nuclear and plasma membranes, in a two-step manner. Firstly, HMGB1 is released into the cytoplasm and later is liberated to the extracellular space. Extracellular HMGB1 can bind to PRRs expressed by myeloid cells like TLR4 and the encompassing advanced glycosylation end-product-specific receptor, which then stimulates processing and cross-presentation of tumor antigens from dying cells. TLR4 activation seems to be indispensable for a cell death to be perceived as immunogenic, with loss of function polymorphisms in the receptor being associated with a worst outcome in patients with breast cancer treated with anthracyclines (Fucikova *et al.*, 2020).

Phosphorylation of eIF2α plays an essential role in ER stress and is considered as a hallmark of the integrated stress response. This event is correlated to the expression of CALR, another important marker for ICD. ER stress is one of the most crucial events in ICD, as illustrated by the exposure of CALR as one of the central DAMPs for inducing immunogenicity. In opposition to this idea, it was found some anthracyclines were found to induce ICD and inhibit features of this phenomenon (Bezu *et al.*, 2018). Additionally, some known inducers, for instance vinca-alkaloids and oxaliplatin do not interfere with ER stress response. Regardless of the stress response, it seems eIF2α phosphorylation for diagnosing immunogenicity, and was observed *in vivo* after treatment with anthracyclines (Bezu *et al.*, 2018), constituting a critical factor and important biomarker for ICD detection.

Heat shock proteins (HSP) function as molecular chaperones for cellular proteins and have cytoprotective and anti-apoptotic effects. Expression of HSP in response to therapeutic agents causing cell death was found to increase tumor cell immunogenicity, with HSP70 exposure followed by HSP90 causing an immunogenic anticancer response (Ahmed; Tait, 2020).

These DAMPs mediate phagocytosis of the dying cells and following antigen presentation on the surface of antigen-presenting cells like DCs. These activated cells then migrate to encounter naive T-cells and present the antigens which are recognized by the T-cell receptor via the presentation on the major histocompatibility complex (MHC) I or II molecules to $CD8^+$ T cells and $CD4^+$ T cells. Naive T-cells also need co-stimulatory molecules, namely CD80 and CD86 to be successfully activated. DCs also deliver signals such as interleukin 12 (IL-12) and IFN assists polarization of T-cells to an IFN-γ-producing phenotype (Ahmed; Tait, 2020).

The current strategies to detect ICD include *in vitro* assessment of DAMP emission in dying cells, but the gold standard is the vaccination assay *in vivo* which evaluates the capability of dying cells to elicit adaptive immunity in immunocompetent syngeneic models, especially mice (Galluzzi *et al*., 2020).

2. RELEVANCE

Even though there are numerous treatments aimed at hematological malignancies present a relevant burden for health systems globally (Keykhaei *et al*., 2021). Occurrence of relapsed and refractory cancer is not unusual and can lead to poor prognosis and overall survival. Targeted therapies are promising immunotherapy tools with specificity that can be used as a strategy to overcome resistance and alleviate adverse side effects. Deregulated pathways related to cell growth, survival, metabolism, and proliferation are linked with several human diseases, constituting targets for pharmacological intervention. The PI3K pathway has major roles in cell signaling and activation of important downstream second messengers and pathways with control over several cellular survival processes. Abnormal PI3K signaling is correlated to many human cancers, with several PI3K inhibitors being developed consequently (Martini *et al*, 2014). Unfortunately, high toxicity and prevalence of low tolerable side effects are some of the critical challenges faced by these molecules, which are usually approved for refractory or relapsed cancers (Yu *et al*., 2023). PI3Kγ expression is enriched in myeloid cells and has promising immunoregulatory activity, with deregulation being associated with immunosuppression (Lanahan; Wymann; Lucas, 2022). Currently, there are no isoform specific PI3Kγ inhibitors approved by the FDA, although some selective molecules have shown interesting anticancer activity and immunological modulation. Enhancing immunogenicity of dying cells is a mechanism linked to therapeutic success and is a strategy for the development of anticancer therapy. Immunogenic cell death is a subtype of regulated cell death in which dying cells expose and liberate molecules which are recognized by dendritic cells to carry out an immune response, perceiving the dying cells as antigenic. Induction of immunogenic cell death has become a desired strategy for the development of novel anticancer molecules and repositioning of off-label drugs (Ahmed; Tait, 2020). In this context, PI3Kγ-inhibitors are promising candidates for the activation of immunogenic biomarkers. Due to difficulties of predicting confidently *in silico* target interaction and structure-activity, phenotypical assessments need to be made to evaluate the biomarkers necessary for ICD. In that manner, the central question of this work was to evaluate if PI3Kγ inhibition is capable of inducing ICD biomarkers *in vitro*.

3. AIMS

3.1 Main aim

To evaluate phenotypic alterations and the presence of selective immunogenic cell death molecular markers induced by PI3Kγ inhibitors in hematological cancer cells.

3.2 Specific aims

- To evaluate the cytotoxic effect of selective and non-selective inhibitors of PI3Kγ in hematologic cancer cell lineages.
- To characterize cytotoxicity of inhibitors in sensitive cell lines.
- To evaluate expression of PI3Kγ by cell lines susceptible to inhibitors
- To assess expression or exposure of immunogenic cell death biomarkers induced by PI3Kγ inhibitors in hematological cancer cells.

4. MATERIALS AND METHODS

4.1 Experimental design

To evaluate the alterations promoted by PI3K, inhibitors were supplied by Professor Alessandra Ghigo at Università di Torino (UNITO). Compounds used were: AS-605240 (PI3K gamma) and IPI-145 (PI3Kγ and PI3Kδ). Different hematological cell lines were chosen for culture and preliminary testing. The murine melanoma cell line B16-F10 was used as a control. Hematological cells used were donated by Professor João Agostinho Machado Neto from University of São Paulo (USP). The B16-F10 cell line was obtained from Rio de Janeiro's Cell Bank (BCRJ).

The hematological cells used were: K562 (human chronic myeloid leukemia), U266 (human multiple myeloma), U937 (human histiocytic lymphoma), Jurkat (human acute T-cell leukemia), RAJI (human Burkitt's lymphoma), WEHI-3B (murine leukemia). Solid cell line B16-F10 (murine metastatic melanoma) was used as a control. Target fishing and evaluation of pharmacokinetics and pharmacodynamics parameters were performed using canonical smiles of the inhibitors of interest. Viability assessment of cells expressing PI3Kγ was performed using the Trypan Blue assay and concentrations for further assays were defined by the results. The colony formation assay was conducted with K562, and Jurkat cells as a control, to gauge if the reduction of viable cells occurs in a cytostatic or cytotoxic manner. Flow cytometry was performed to assess the immunogenic cell death markers involved in PI3Kγ inhibition. Cell membrane integrity and morphology was appraised in K562 cells incubated previously with inhibitors for 24 hours. Treated cells were also photographed to observe the qualitative changes associated. Lastly, western blot was conducted to analyze key protein expression. Main steps of the experimental design are portrayed in **Figure 4**.

Figure 4 - Principal steps of the experiment design. Illustration (a) of the principal processes and experiments involved in the present work.

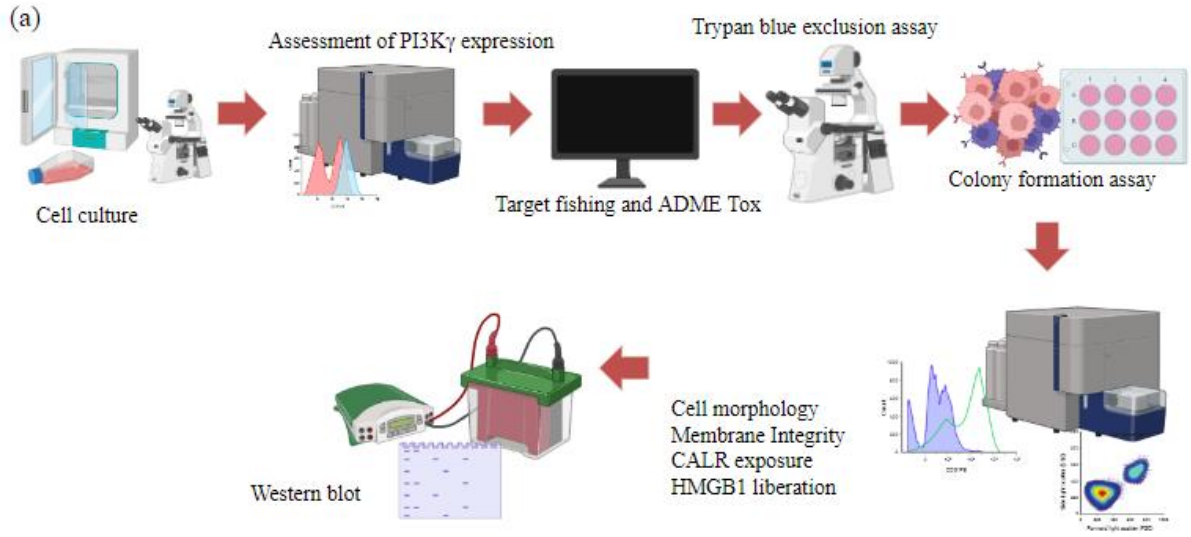

Source: Made by author using Bio Render.

Illustration (a) of the principal processes and experiments involved in the present work.

4.2 Cell Culture Protocols

Cell lines described in the experimental design section were cultivated for further experimentation. The mediums used were Roswell Park Memorial Institute (RPMI) 10% Fetal Bovine Serum (FBS) for K562, U266, U937, JURKAT, RAJI cell lines, Iscove Modified Dulbecco Media (IMDM) with 20% FBS supplementation for WEHI-3B cell line and Dulbecco's Modified Eagle Medium (DMEM) 10% FBS for B16-F10 cell line. Cells were cultivated in plastic flasks for culture (Corning, 25 $cm^{2,}$ 50 mL or 75 cm^2, 250 mL). All mediums used were supplemented with FBS and 1% antibiotic (100 µg/mL penicillin and 100 µg/mL streptomycin) (Gibco). Cells were handled in vertical laminar flow cabin (ESCO, model Airstream class II-B2; VECO, model Biosafe 12 class II) and kept in CO_2 5% incubator at 37°C (SAYNO, model MCO-19AIC; NUAIRE, TS Autoflow). The growth and morphology of the lineages was monitored daily with the aid of inverted optical microscopy (LABOMED, TCM 400; Nikon, model Diaphot). When needed, cell medium was exchanged. For the adhered cell model, trypsin-EDTA 0,5% (Gibco) diluted in 10X Phosphate Buffered Saline (PBS).

4.3 Evaluation of PI3Kγ expression by Flow cytometry

To assess the presence of PI3Kγ the cells lines described previously (K562, U266, U937, JURKAT, RAJI, WEHI-3B and B16-F10) were cultured and plated in 24-well plates at

the concentration of $2x10^5$ cells per mL. Immediately after, begin the procedure of washing and prepping the cells for intracellular marking. The content of the wells was moved to eppendorfs which were centrifuged at 1500 RPM, for 5 minutes at 4°C, the supernatant was discarded, and the pellet was washed with 300 µL of paraformaldehyde in 4% PBS. The eppendorfs were left to incubate for 5 minutes in the dark (room temperature) then centrifuged and the supernatant discarded again.

After, 200 µL of tríton 0,1% was added and incubated for 5 minutes at room temperature. Cells were centrifuged and the supernatant discarded again, cells were washed with FACS 4% buffer and centrifuged once more. At that point, 10 µL of the antibody PI3K p110γ (Cell Signaling) in concentrations ranging from 1:100 to 1:300 and 10 µL of FACS 4% were added. Cells were left incubating in ice for 40 minutes protected from the light. After incubation, cells were washed and centrifuged. To detect the primary antibody, a secondary antibody Anti-Rabbit coupled with Alexa-488 was used for flow cytometry visualization. The antibody was diluted in a range from 1:1000 to 1:3000 for titration, and 10 µL of the dilution was added with 10 µL FACS 4% and incubated for 40 minutes in the ice protected from light.

The DAPI (4′,6-diamidino-2-phenylindole) dye was used to confirm intracellular marking. DAPI is a fluorochrome with the capacity of forming a DAPI-DNA complex, which can only bind to double stranded DNA if the plasma membrane is already permeabilized. Thus, DAPI can be used as a control fluorescence dye for the permeabilization process (HAMADA; FUJITA, 1983). After antibody incubation, the cells were resuspended in a solution 300 µL of a FACS 4% and DAPI 2 µg/mL and kept incubating protected from the light for 5 minutes. Unmarked cells were resuspended in 200 µL FACS 4%. Samples were acquired in a FACSVerse (BD Biosciences) cytometer. The Fluorescence count graphs were plotted using the FlowJo Image Analysis software. Gates strategy used is described by **Figure 5** below.

Figure 5 - Gates strategy for detecting PI3Kγ expression via flow cytometry

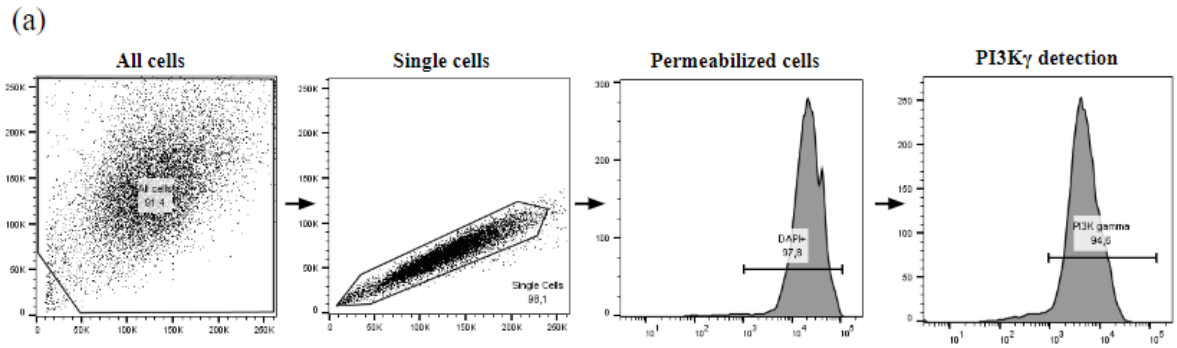

Source: Made by author.

From the All cells gate, the single cells gate is created. From single cells, a histogram gate for permeabilized cells is created using DAPI fluorescence. From permeabilized cells is created the histogram for PI3Kγ detection using Alexa-488's fluorescence.

4.3 Target Fishing and ADME Tox

To assess absorption, distribution, metabolism and toxicity (ADME Tox) parameters, the canonical smiles of AS-605240 (CID 5289247) and IPI-145 (CID 50905713) were collected from PubChem and submitted to SwissADME, a free online tool (Daina; Michielin; Zoete, 2017) that also predict models of pharmacokinetics, drug-likeness, and chemical properties.

Drug-likeness is a concept based on the work of Lipinski and refers to the possibility of a compound to be an orally administered drug. Targets with the highest probability were selected as the most interesting. For comparison of most probable targets the free tools SwissTargetPrediction and PassTargets were also used.

4.4 Viability assessment using Trypan blue exclusion assay

To measure cell viability after exposure to the PI3K inhibitor, the trypan blue exclusion assay was used. Trypan Blue is a dye capable of selectively penetrating the cytoplasm of non-viable cells. In this protocol, non-viable cells would be stained blue and viable cells would be able to expel the dye, being clear colored. Cells were plated in 96-well plates in concentration of 1 x 10^5 cells/mL. The inhibitors tested were AS-605240 and IPI-145 in logarithmic dilution (3 µM, 1 µM, 300 nM, 100 nM, 30 nM). The exposure to the molecules lasted for 24 hours. The assay was performed as described by Strober, 2015 (Strober, 2015). The percentage of viable cells was obtained using the formula shown below:

Equation 1 – Viable cells calculation for trypan assay.

$$\text{viable cells } (\%) = \frac{\text{total number of viable cells per ml of aliquot}}{\text{total number of cells per ml of aliquot}} \times 100$$

Source: STROBE, 2015.

Data was plotted using GraphPad Prism 8.0 and analyzed via one-way ANOVA and Dunnett's post-test ($P < 0.05$).

4.5 Colony formation assay

K562 and Jurkat cells were seeded at a concentration of $1x10^3$ cells per milliliter in methylcellulose medium for human cells (MethoCultTM H4230, STEMCELL Technologies) in a 12-well plate. Then, treatments of 0.1, 0.3, 1 and 2µM of each inhibitor were administered, as well as 1µM of Dox. RPMI medium was used as negative control. After 24 hours of exposition to treatments, the content of the wells was substituted by culture cell medium. Plates were observed for the formation of colonies every two days. After 11 days the experiment was stopped, the content of the wells was washed with PBS and 0,5% crystal violet in 50% methanol. Plates were washed with distilled water for dye removal and plates were scanned. Colony count was performed using ImageJ. Numbers were then plotted using GraphPad Prism 8.0 and analyzed through one-way ANOVA and Dunnett's post-test with p-value <0.05.

4.6 Cell death analysis by Flow cytometry and cell imaging

Flow cytometry is a robust technique for the assessment of different parameters in individual cells. Cells or particles are analyzed as they pass lasers while suspended in a buffered saline solution. The laser scatter can be measured in two directions, forward (FSC) and side scatter (SSC). The FSC correlates to cell size as the SSC does to volume or internal complexity. Samples can also be prepared using dyes or stained using fluorochrome conjugated antibodies that can be excited by the equipment's lasers (McKinnon, 2018). The cytometers used for the following experiments were the FACSVerse (BD Biosciences) and the Attune (ThermoFisher Scientific).

For live-cell imaging, K562 cells were prepped, incubated with treatments for 24 hours and marked with DAPI (4′,6-diamidino-2-phenylindole) for nuclei visualization. Images were captured using the Cytation^{TM} 3 Cell imaging Multi-Mode Reader (Biotek) at 20x magnification.

4.6.1 Cell prepping

For the cytometry experiments, K562 cells lines were seeded at $2x10^5$ cells/mL in 24-well plates and exposed to AS-605240 and IPI-145 in concentrations of 0.3 and 1µM for 24 hours. DOX 1µM and DMSO were used as positive and negative controls, respectively, for the same period. After the 24 hours, the content of each well was transferred to a microtube and centrifuged for 1500 RPM, 5 minutes at 4 °C. The supernatant was discarded, and the pellet was resuspended in a FACS 4% solution (saline solution containing 4% of FBS). The details ascertaining to each protocol are described below.

4.6.2 Gates strategy and data analysis

After proper sample staining, 10 thousand events (after debris and doublets removal) were acquired for all experiments. Firstly, a morphology graph (dot plot) was created using the FSC and SSC parameters containing all the particles acquired (all events). In this graph, a selection region was created to exclude debris and outliers, creating all cells plot. From all cells a gate was created to exclude doublets, which results in the single cells graph. To obtain single cells, the FSC parameter is plotted in both axis (FSC-H vs FSC-A). These graphs are common to all cytometry experiments, and from the single cells plot other graphs can be derived.

The data obtained via flow cytometry was analyzed using the FlowJo (Star Tree Inc) software. Median fluorescence intensity (MFI) values were obtained in FlowJo and normalized using the mean values of the negative control. Statistical analysis was performed using the GraphPad Prism 8.0 software. To evaluate statistical significance between groups, data was analyzed by one-way ANOVA and Dunnett post-test, with 5% ($p < 0,05$) significance.

4.6.3 Cell Morphology

The cell morphology changes observed after exposure to a molecule are important signals of what is occurring to cells in consequence of the interaction. Cells were washed and prepped in microtubes for flow cytometry acquisition. For this analysis fluorochromes were not required since morphological characteristics can be assessed using the laser's FSC and SSC dispersion. The FSC correlates to size and cell volume and SSC correlates to internal complexity or granulosity. Data obtained from the cytometer was analyzed in FlowJo. Statistical analysis was performed using the GraphPad Prism Software.

4.6.4 Membrane integrity

Plasma membrane integrity is essential to normal cell function. When cells are in the process of dying or dead, membrane integrity can be lost. To evaluate the membrane integrity the fluorochrome DAPI (4′,6-diamidino-2-phenylindole) was used. It can emit fluorescence upon binding with AT regions of DNA and can only bind to DNA in cells with permeable or ruptured plasma membranes. The DAPI dye is excited by the violet laser in the range of 355 nm and emits at about 457 nm. When the fluorescence is detected, it shows that a cell population has lost its membrane integrity, and as such are non-viable cells.

After cell washing and prepping, the pellets were resuspended in 300 µL of FACS 4% and DAPI at 2 µM/mL. The cells were left incubating in the dark for 5 minutes and then samples

were acquired by flow cytometer. The emission intensity correlates to the percentage of cells which lost their membrane integrity. Data obtained was analyzed in the FlowJo software and statistical analysis was performed using the GraphPad Prism.

4.6.5 Evaluation of HMGB1 release

HMGB1 liberation is one of the most important hallmarks of ICD. To assess this event, a specific antibody for the HMGB1 protein and conjugated to the phycoerythrin (PE) fluorochrome (PE anti-HMGB1; Biolegend) was used. PE is excited at 564 nm and emits yellow fluorescence at 574 nm. Considering HMGB1 is a nuclear protein, cells must be permeabilized to allow the antibody to bind to the target. If the protein is being liberated, the treated groups must have a lower signal than the negative control group.

After cells were prepped, they were fixated with a paraformaldehyde solution (PFA 0,4%). Following, cells were washed with FACS 4% and permeabilized with Triton-X 100 0,1% for 5 minutes. Succeeding, cells were washed and incubated with PE anti-HMGB1 (1:100) for 40 minutes in ice and in the dark. In the end, cells were washed with 300 μL FACS 4% to be acquired by cytometer. Mitoxantrone was used as the positive control, as doxorubicin interferes with PE-signal. Cytometry archives were analyzed in FlowJo software, with gate strategy shown in **Figure 6**, and PE's MFI values were normalized by the negative control. Data obtained was analyzed through one-way ANOVA with Dunnett's multiple comparisons post-test in GraphPad 8.0.

Figure 6 - Gates strategy for HMGB1 liberation.

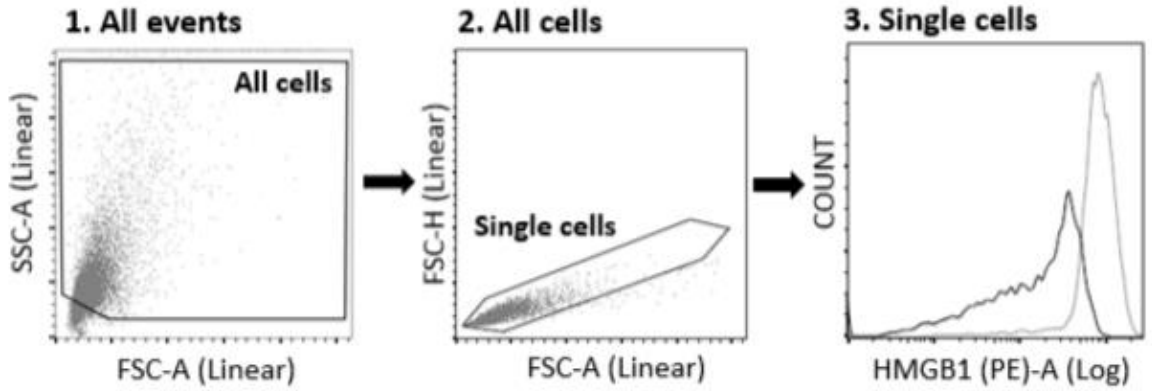

Source: Elaborated by the author.
From the single cells gate, a histogram was created with the fluorescence filter for PE to verify HMGB1 liberation, in a manner that a decrease in fluorescence when compared to control groups show HMGB1 liberation occurred. The PE MFI values were used for statistical analysis. The histogram lined in black refers to a sample that is reducing PE signal, and the histogram with lighter tracing refers to negative control.

4.6.6 CALR exposure

CALR exposure is one of the key events in ICD (Obeid *et al*., 2006). To evaluate this phenomenon, a specific Anti-CALR (Calreticulin (D3E6) XP Rabbit mAb, Cell Signaling) antibody was used. For the fluorescence, a secondary antibody (anti-rabbit) conjugated with Alexa Fluor 488 was used. Alexa Fluor 488 is excited at 493 nm by the blue laser and emits green fluorescence at 518 nm. CALR exposure occurs in the plasma membrane, and as such DAPI dye was used as a control of membrane integrity. Only viable cells are of interest for the detection of CALR. Gate strategy for this experiment is shown on **Figure 7**.

For the assay, after cells were prepped, they were left incubating with anti-CALR (1:300) in the ice for 40 minutes in the dark. Afterwards, the cells were washed and incubated with Alexa Fluor 488 (1:400) for 40 minutes in the ice and in the dark. Cells were washed and incubated with DAPI at 2 μM/mL for 5 minutes. Flow cytometry archives were analyzed with FlowJo and statistical analysis was realized using GraphPad Prism. Statistical analysis was performed using MFI values for Alexa Fluor 488.

Figure 7 - Gates strategy for CALR externalization analysis.

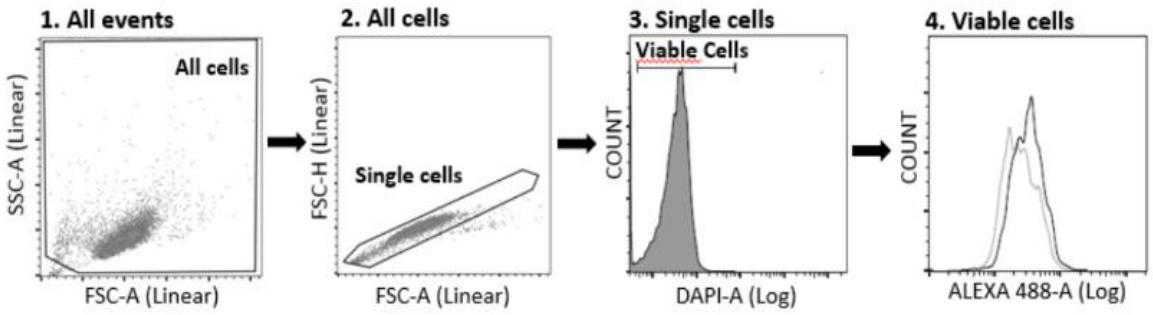

Source: Elaborated by the author.
A histogram was created through the single cells gate to verify viable cells from DAPI fluorescence. This population was selected from the viable cells gate. A new histogram was created from the viable cells gate to verify CALR externalization through Alexa 488 fluorescence intensity. MFI values were used in the software GraphPad Prism to compare differences between groups.

4.7 Western Blot

Western blot is a method for detection and quantification of proteins using specific antibodies. Firstly, K562 and Jurkat cells were seeded in cell culture plates at a concentration of $1x10^3$ cells per milliliter in methylcellulose medium for human cells (MethoCultTM H4230, STEMCELL Technologies) in a 12-well plate. They were incubated with RPMI medium

(negative control), DOX 1 μM, AS-605240 and IPI-145 at 0.1, 0.3 and 1μM for 24 hours. Total protein extraction was performed in a buffer containing 100 mM Tris (pH 7.6), 1% Triton X-100, 150 mM NaCl, 2 mM PMSF, 10 mM Na3VO4, 100 mM NaF,10 mM Na4P2O7, and 4 mM EDTA. Extracted proteins were quantified using the Bradford method. Equal amounts of protein were used for SDS-PAGE protein separation and subsequent blot analysis as described by Lima *et* al., 2019. The percentage of the polyacrylamide gels ranged from 8 to 15% and nitrocellulose membranes (GE Healthcare) were used. The α-tubulin was used as the loading control. Secondary antibodies anti-mouse (cat. no. 7076) and anti-rabbit (cat. no. 7074) conjugated with horseradish peroxidase were obtained from Cell Signaling Technology, Inc. and used in the 1:2000 dilution with 2h of incubation. Antibody binding was revealed using a substrate system SuperSignalTM West Dura Extended Duration (Thermo Fisher Scientific) and the gel imaging was developed using G: BOX Chemi XX6 (Syngene, Cambridge, UK) documentation system. After development and image capture, values were obtained for each band. Numerical data was obtained from each sample tested by relative density. A list of antibodies used can be found in **Table 1**.

Table 1- List of antibodies tested in western blot and their specifications.

Antibody	Manufactory	Cat. number	Experiment
PARP1	Cell Signaling	#9542	Tested
p-eIF2 α	Cell Signaling	#9721	Tested
eIF2 α	Cell Signaling	#9722	Tested
p-RPS6	Cell Signaling	#4858	Tested
RPS6	Cell Signaling	#2217	Tested
LC3B	Cell Signaling	#2775	Tested
SQSTM1/p62	Cell Signaling	#88588	Tested
α-tubulin	Cell Signaling	#2144	Tested

Source: Obtained from Dr. Anali Garnique and Dr. João Machado-Neto.

Quantitative values were generated for each gel band using UN-SCAN-IT gel 6.1 software. Phosphorylated eIF2α values were divided by the values obtained for eIF2α and then normalized with negative control results. The same was done for phosphorylated S6RP and the correlation for cleaved and non-cleaved PARP-1. LC3B and p62 values were divided by α-tubulin values and normalized using negative control. Data was plotted using GraphPad Prism 8.0.

5. RESULTS

5.1 Evaluation of PI3Kγ expression by Flow cytometry

PI3Kγ expression was evaluated using flow cytometry and analyzed using the FlowJo software. The histograms were generated for each cell type. As PI3Kγ is constitutively enriched in myeloid cells, expression was expected of cell lines derived from myeloid progenitors. Of all lineages tested (K562, U266, U937, Jurkat, RAJI, WEHI-3B and B16-F10), K562 was the only one to present clear expression of PI3Kγ, as shown by **Figure 8**.

Figure 8 - Detection of PI3Kγ expression in different cell lines. Histograms demonstrating PI3Kγ expression (in blue) by K562 (a), Jurkat (b), B16-F10 (c) cell lines against non-marked control (in red).

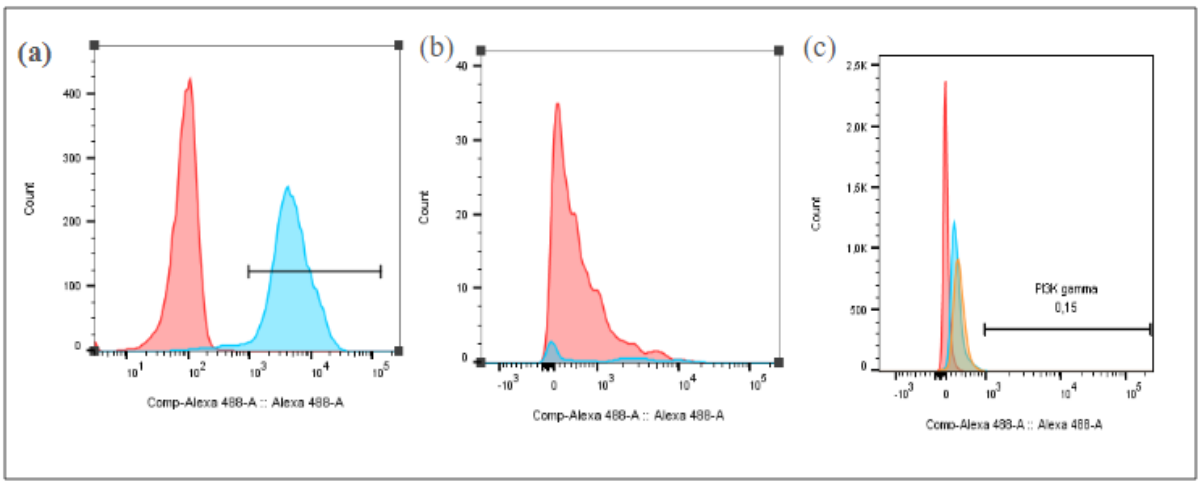

Source: Made by author.

5.2 Target Fishing and ADME TOX

To evaluate possible targets and pharmacological parameters of the PI3Kγ inhibitors, the canonical smiles of AS-605240 and IPI-145 were submitted to SwissADME, SwissTarget and PassTargets, free online tools used for target prediction.

For IPI-145 the results predicted that the molecule is moderately soluble in water, with high gastrointestinal absorption and incapable of penetrating the blood-brain barrier. It also constitutes a P-glycoprotein substrate and an inhibitor of CYP2C19, CYP2C9 and CYP2D6. It also passed the drug-likeness category based on Lipinski, Ghose, Veber, Egan and Muegge with a bioavailability score of 0.55. Other than the predicted targets associated to PI3Kγ/δ the tools showed Tyrosine-protein kinase FYN and Serine/threonine-protein kinase TNNI3K as binding targets.

For AS-605240, the selective inhibitor of PI3Kγ, SwissADME results predicted solubility in water, high gastrointestinal absorption and CYP1A2 inhibition. The molecule also passed drug-likeness parameters-based Lipinski, Ghose, Veber, Egan and Muegge with a bioavailability score of 0.55. Other possible targets reported were Tyrosyl-DNA phosphodiesterase 1, Serine/threonine-protein kinase haspin.

5.3 Viability assessment using Trypan blue exclusion assay

K562 cells treated with AS-605240 and IPI-145 at 3000, 1000 nM and 300 nM concentration showed antiproliferative effect when compared to negative control.

Figure 9 - Viability of K562 cells after exposure to inhibitors AS-605240 and IPI-145.

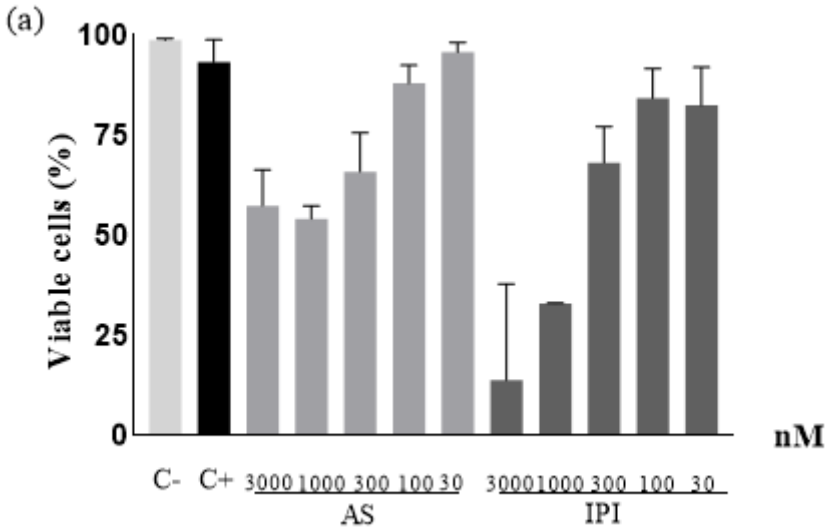

Source: Made by author.

The figure above (a) shows the percentage of viable cells for negative and positive control, and the inhibitors in concentrations ranging from 3000 to 30 nM. N=1 with three replicates for each group. Negative control (C-)

To avoid off-target pharmacological interactions, the 3 μM concentration was excluded from following experiments. The 30 nM concentration was also excluded due to the lower toxicity.

5.4 Colony formation assay

For the colony formation assay K562 and Jurkat cells were seeded and exposed to AS-605240 and IPI-145. Plates were monitored visually every two days until control wells were

totally occupied by colonies. Total experiment time amounted to 11 days. Plates were then scanned, and colonies were counted using ImageJ software. Values were plotted on GraphPad Prism 8.0 and analyzed in one-way ANOVA. The DOX wells showed practically no colonies after the experiment incubation period for K562 and Jurkat cells. For K562 cells, the specific inhibitor AS-605240 reduced the number of colonies at the concentrations of 2000 and 1000 nM when compared to negative control. Even though viability was reduced by the inhibitors, the reduction of colonies was attributed to a cytostatic effect, since many factors could alter cell viability without necessarily meaning cell death. Exposure to IPI-145 reduced colonies of K562 cells at the 300, 1000 and 2000 nM concentration. The discrete reduction of colony count was also attributed to a cytostatic effect.

Figure 10 - Colony formation assay in K562 cells.

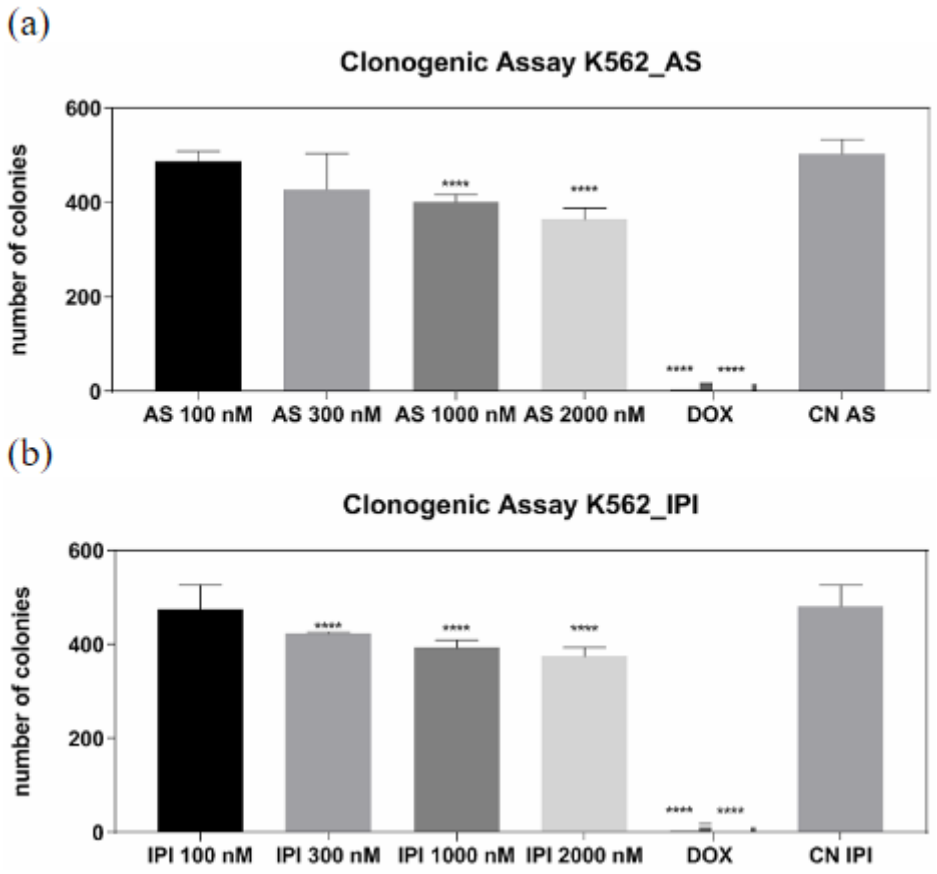

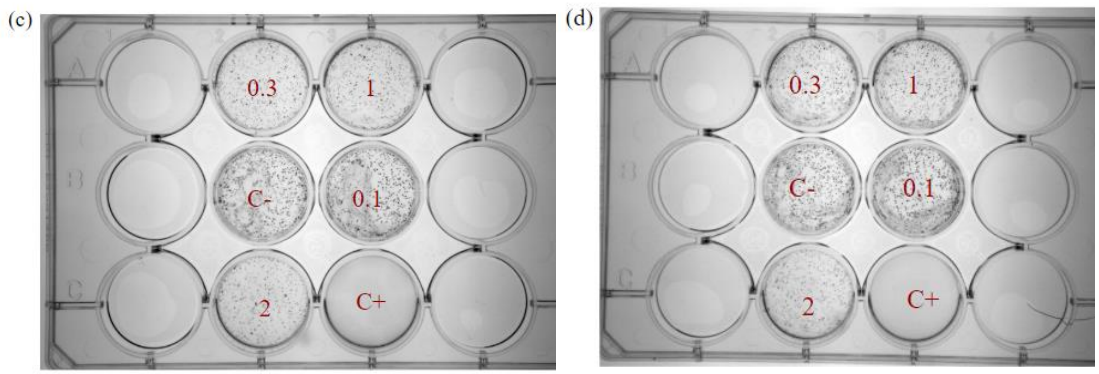

Source: Made by author.

Graphs show the number of colonies for K562 cells exposed to AS-605240 (a) and IPI-145 (b). Significant difference from negative control is illustrated by asterisks. The groups AS 1000, 2000 nM and DOX were able to reduce the number of colonies when compared to negative control. After 11 days the plates that were incubated with AS-605240 (c) and IPI-145 (d) were scanned and colonies were counted using ImageJ software. Values were plotted in GraphPad Prism 8.0 and analyzed in one-way ANOVA with Dunnett's post-test (P <0.05). N=3.

For Jurkat cells, both AS-605240 and IPI-145 were capable of reducing the number of colonies only at the highest concentration tested (2000 nM).

Figure 11 - Colony formation assay in Jurkat cells.

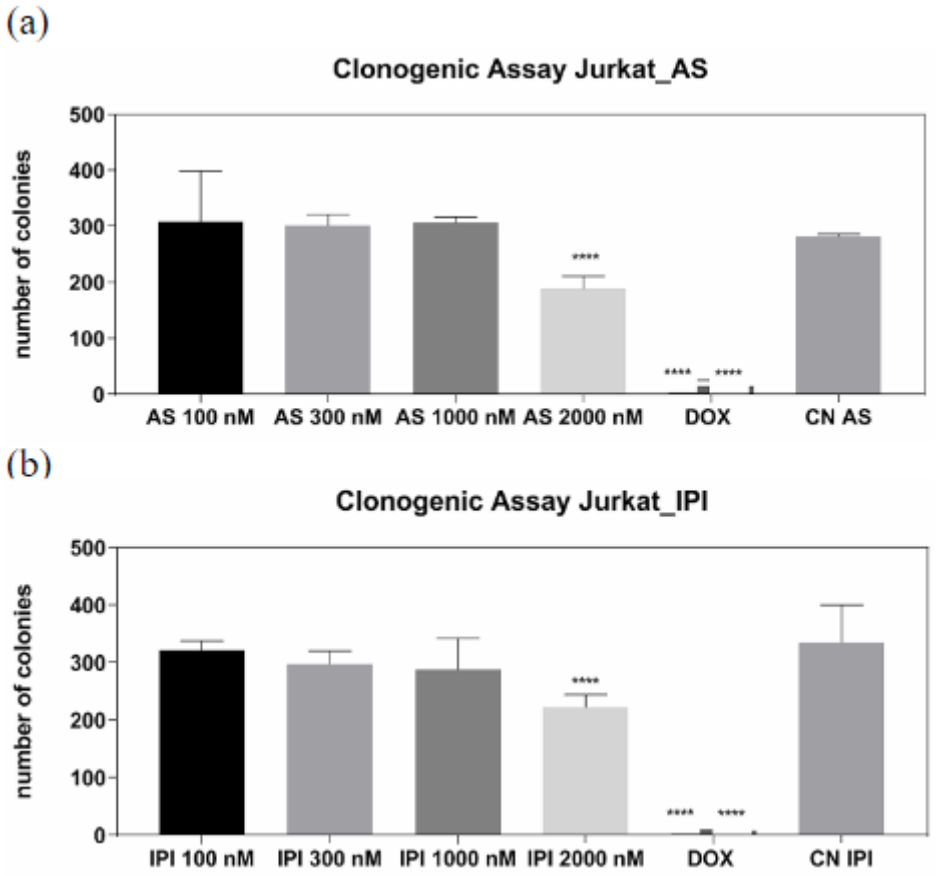

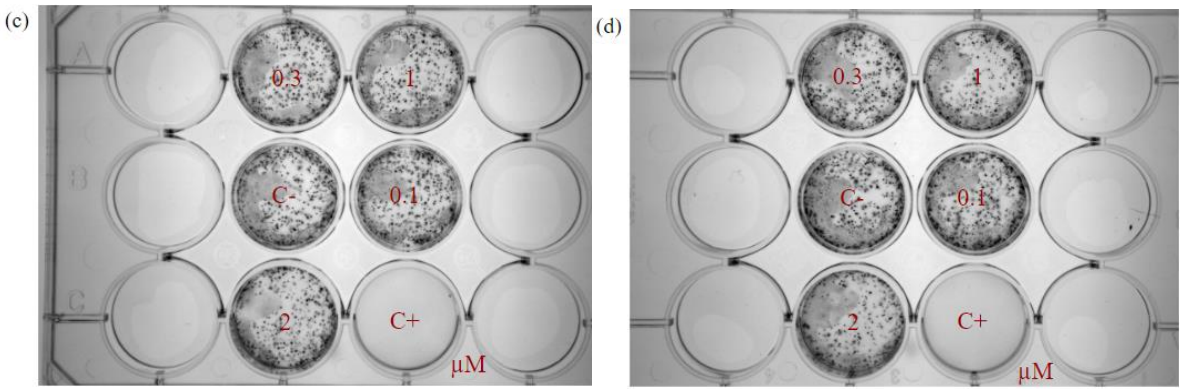

Source: Made by author.

Graphs show the number of colonies for Jurkat cells exposed to AS-605240 (a) and IPI-145 (b). Significant difference to negative control is illustrated by asterisks. The groups AS 2000, IPI 2000 nM and DOX showed reduction of the number of colonies when compared to negative control. Plates of Jurkat cells after incubation with AS-605240 (c) and IPI-145 (d) were scanned and the number of colonies was counted using ImageJ software. Values were plotted in GraphPad Prism 8.0 and analyzed through one-way ANOVA and Dunnett's post-test ($P < 0.05$). N=3.

5.5 Cell Morphology

Both AS-605240 and IPI-145 at 1000 nM were able to induce significant cell morphology changes such as, increase in shrinking and high granularity cells when compared with negative control. Positive control was also able to induce significant alterations (**Figure 12**). Cell morphology gates were established according to negative control and maintained for all morphology experiments. Live-cell images were generated to visualize cells after 24-hour incubation. In the negative control images, it is possible to visualize that the K562 nucleus appears round and individualized. In the treated groups, pyknosis and nuclear fragmentation are noted.

Figure 12 – Evaluation of cell morphology in K562 cells.

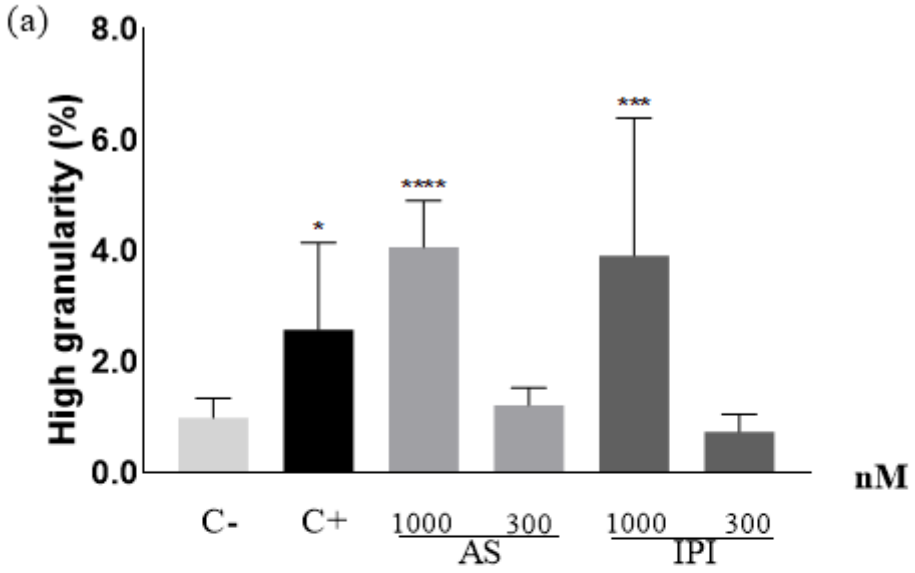
(a)
8.0
6.0
4.0
2.0
0.0
High granularity (%)
*
****
***
nM
C-
C+
1000
300
AS
1000
300
IPI

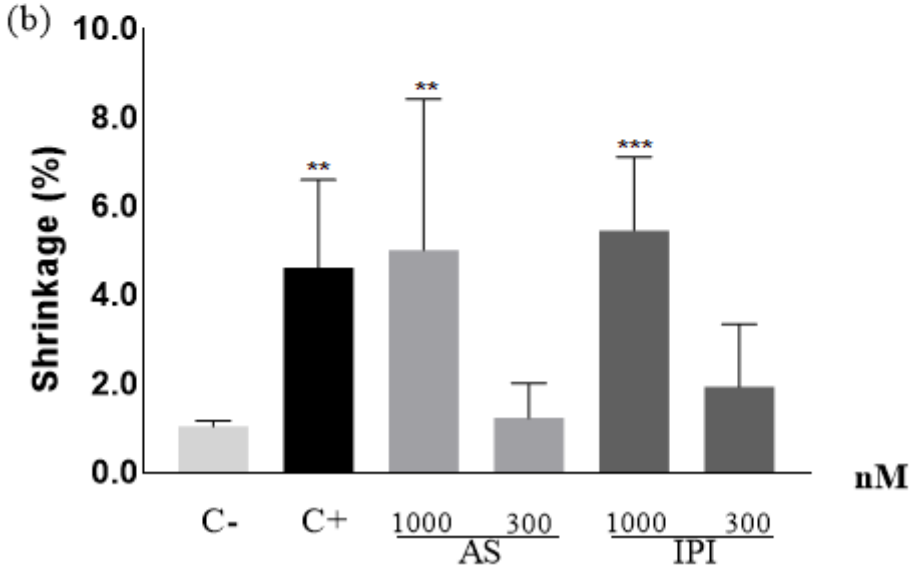
(b)
10.0
8.0
6.0
4.0
2.0
0.0
Shrinkage (%)
**
**
***
nM
C-
C+
1000
300
AS
1000
300
IPI

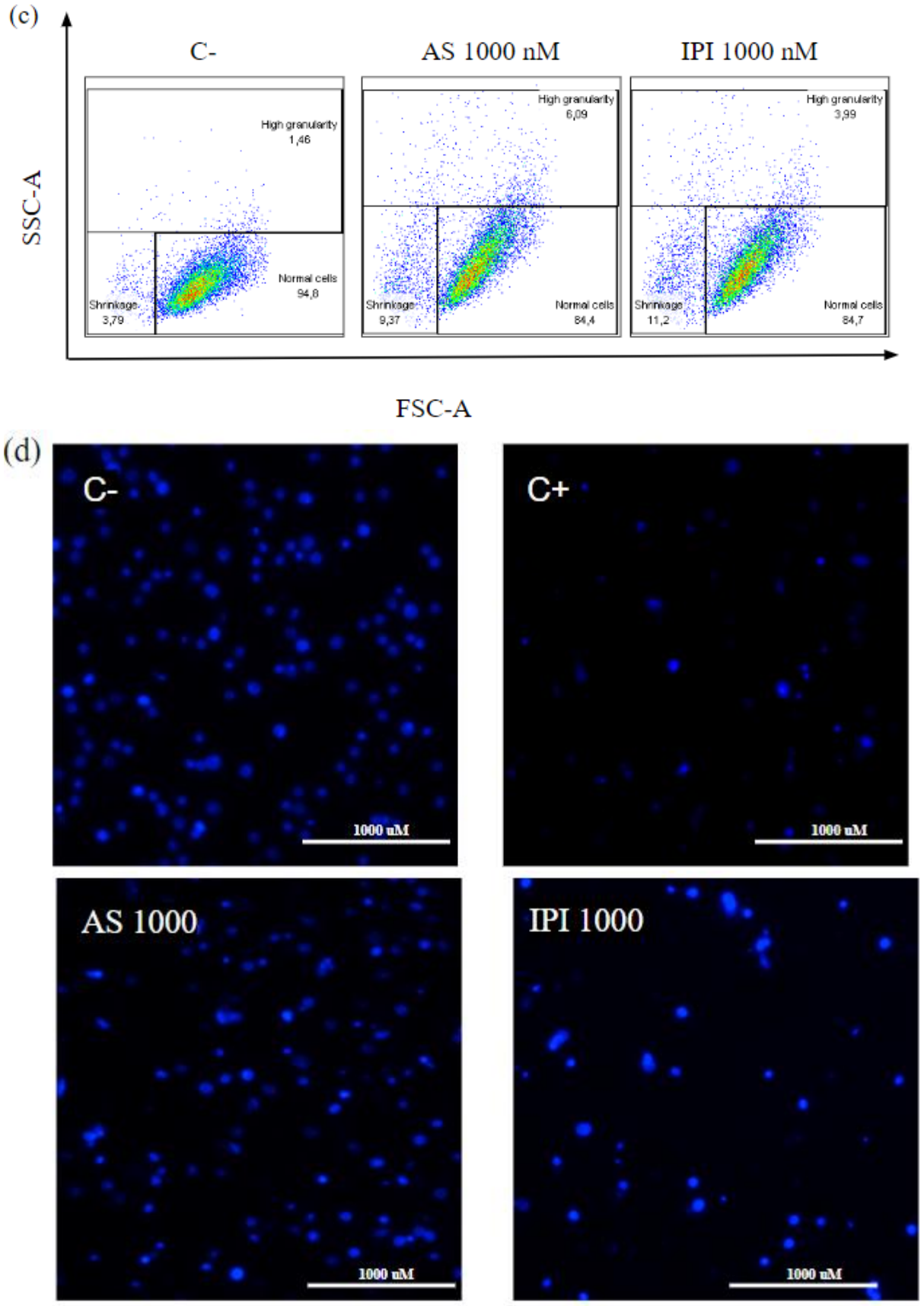

Source: Made by author.

Morphology of K562 cells incubated with Dox 1000 nM, AS-605240 1000 nM and 300 nM, IPI-145 1000 nM and 300 nM for 24 hours. Percentage of high granularity cells (a) and shrinking cells (b). Representative flow cytometry dot-plots are shown (c) for negative control, AS-605240 and IPI-145 1000 nM. N=3. ($p<0.05$) Live-cell images (d) were obtained using Cytation™ 3 and the nuclei of cells appear in blue. The images show stained cells after incubation with negative and positive control, as well as inhibitors AS-605240 at 1000 nM.

5.6 Membrane integrity

Membrane integrity is a parameter for assessing the number of viable or non-viable cells. Only IPI-145 at 1000 nM concentration was able to increase significant loss to membrane integrity (**Figure 13**)

Figure 13 - Evaluation of membrane integrity.

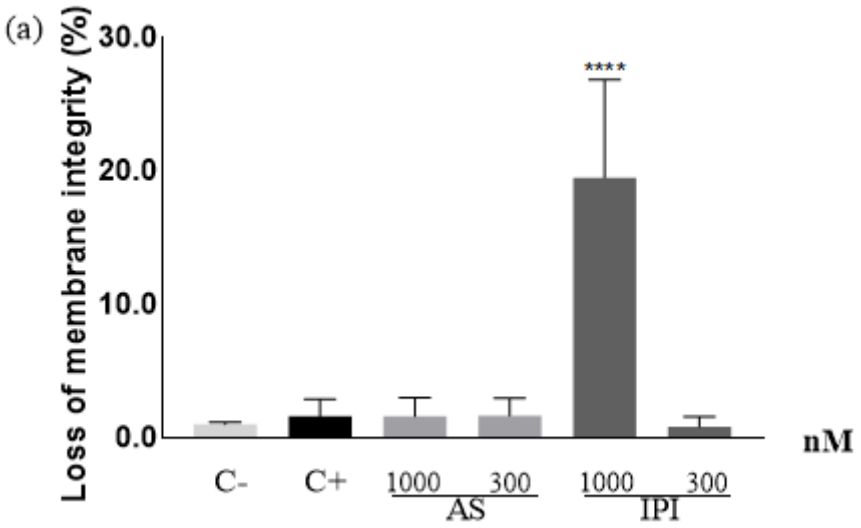

Source: Made by author.
Graph (a) shows percentage of cells with ruptured membrane after 24 hours exposure to PI3K**γ** inhibitors. N=3. ($p<0.05$)

5.7 Evaluation of HMGB1 release

HMGB1 release from the nucleus to the extracellular medium can be perceived by the reduction in PE fluorescence, the fluorochrome that is attached to the anti-HMGB1 antibody. MFI values were normalized using negative control data. Only the mitoxantrone (positive control) was able to reduce HMGB1 signal, while AS-605240 and IPI-145 actually increased PE's MFI, as showed by **Figure 14**.

Figure 14 - Nuclear HMGB1 by K562 cells exposed to PI3Kγ.

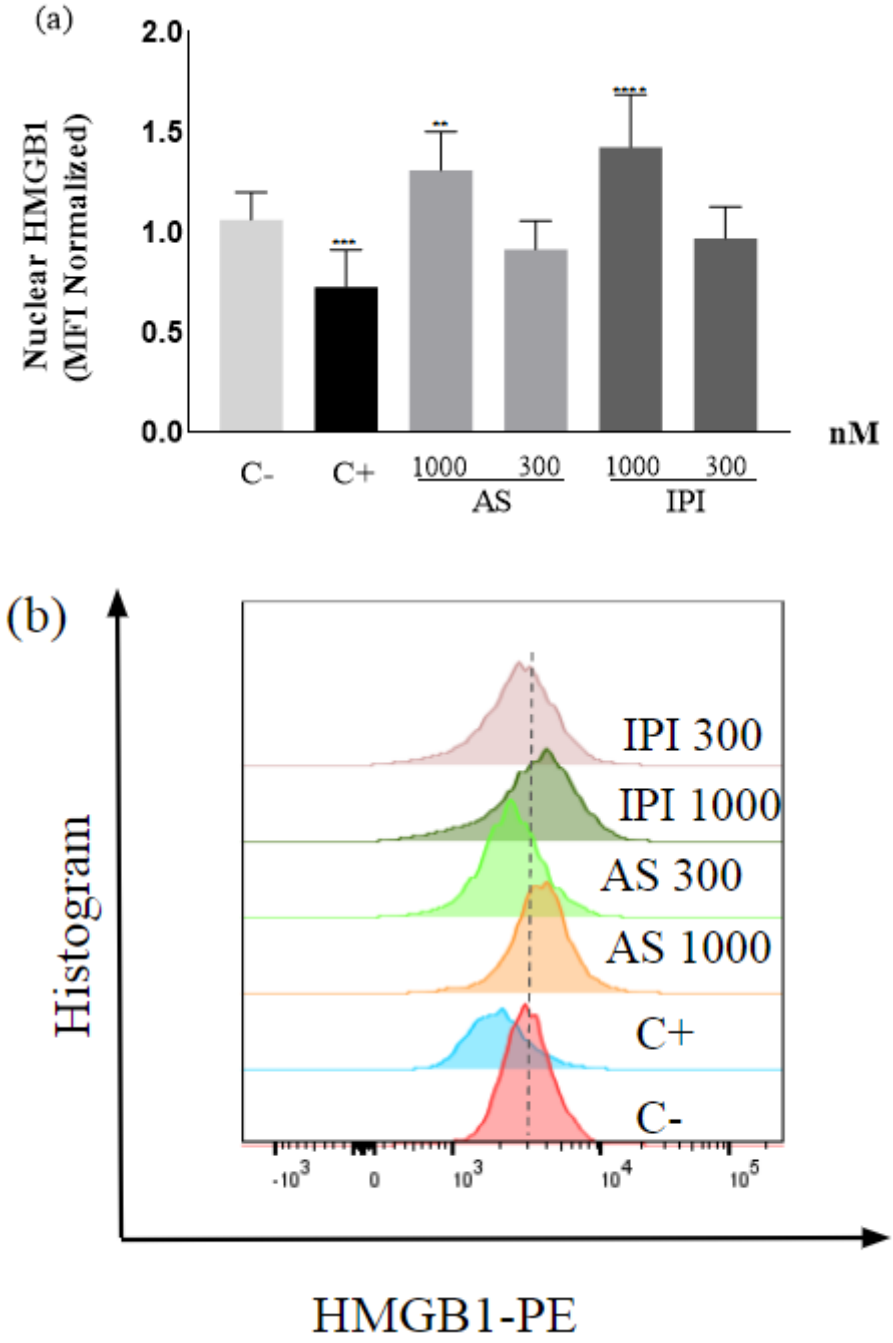

Source: Made by author.

Graph illustrating alterations in nuclear HMGB1 (a) with DOX showing a reduced signal for HMGB1 which correlates with HMGB1 liberation, and AS-605240 and IPI-145 at 1000 nM increasing the signal, and consequently increasing intracellular HMGB1. Representative histograms (b) are shown for negative and positive control, AS-605240 at 300 and 1000 nM, and IPI-145 at 300 and 1000 nM. N=4, ($p<0.05$).

5.8 CALR exposure

Cells incubated with the inhibitors, as well as the positive control DOX were able to increase CALR exposure, as illustrated by the increase in the MFI of Alexa-488 (**Figure 15**), in all concentrations tested when compared with negative control.

Figure 15 - Calreticulin exposure of K562 cells exposed to PI3K inhibitors.

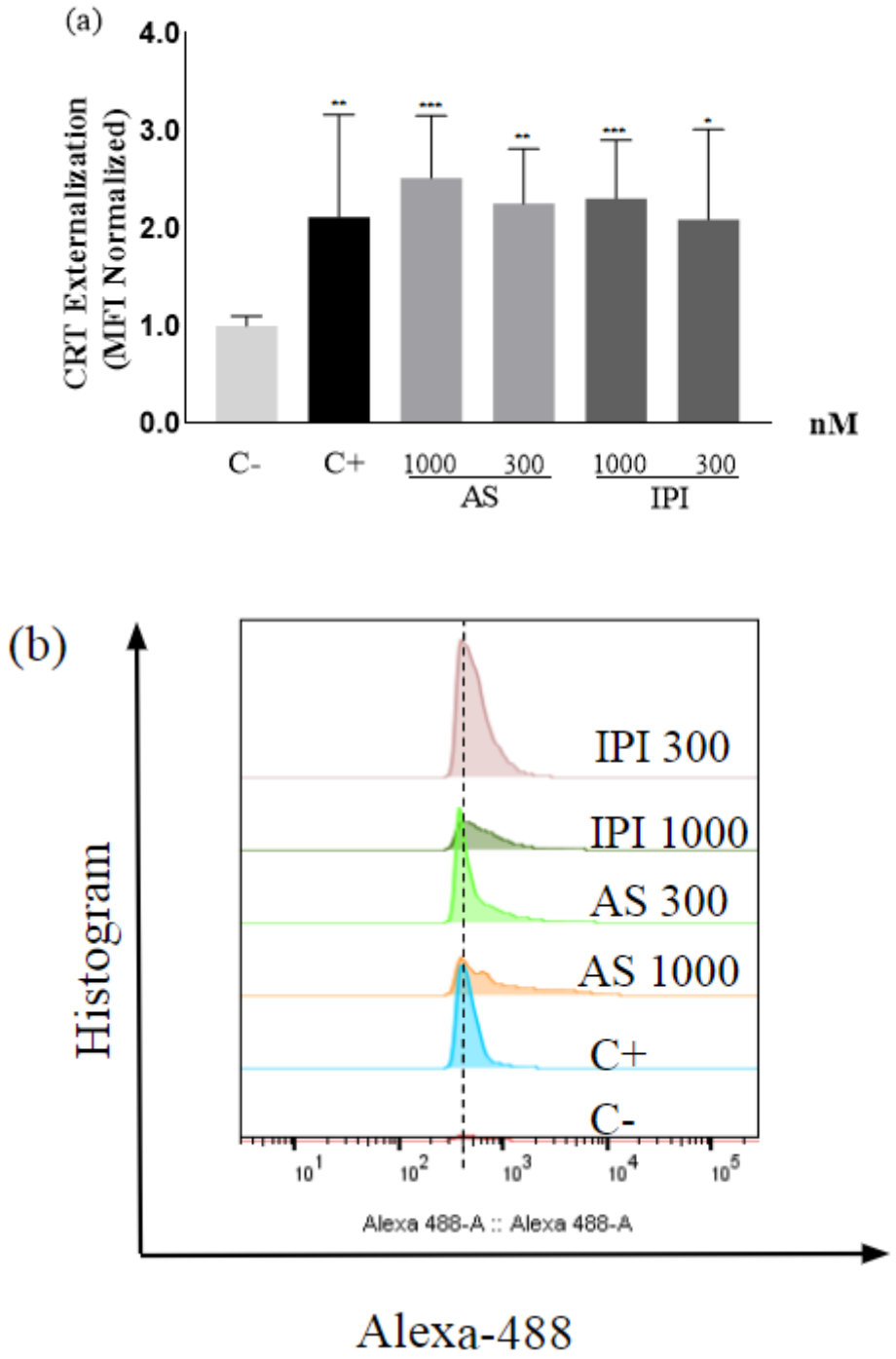

Source: Made by author.

K562 cells were seeded and incubated with the inhibitors for 24 hours. CALR exposure was measured by the MFI of the fluorochrome Alexa-488. Analysis shows that all experimental groups were able to induce significant CALR exposure. MFI values of Alexa-488 were normalized (a) and compared to negative control by one-way ANOVA and Dunnett post-test. Calreticulin exposure was clearly observed even at the 300 nM concentration, as displayed by the histograms presented (b) AS-605240 300 and IPI-145 300 and 1000 nM. N=3.

5.9 Western Blot

For the western blot assay, several proteins were evaluated. For K562 cells, all treatments reduced the cleaved PARP-1/PARP-1 (**Figure 16a**.) ratio when compared to negative control. In K562 cells, DOX, AS 100 nM, AS 1000 nM and all concentrations of IPI-145 (100, 300 and 1000 nM) were able to increase levels of phosphorylated eIF2α (**Figure 16a and 16b**) when compared to negative control, with AS 100 nM presenting the highest increase. Inhibitors and DOX reduced the levels of phosphorylated S6RP, a downstream target of the PI3K pathway in K562 cells (**Figure 16a and 16c**). For p62 levels, DOX and all tested concentrations of AS-605240 increased values, as cells treated with IPI-145 showed substantial decrease (**Figure 16b and 16g**). K562 cells treated with DOX and AS 1000 nM had increased levels of LC3B, while cells treated with AS 100 nM, AS 300 nM and all concentrations of IPI-145 had decreased expression (**Figure 16b and 16h**).

For Jurkat cells, only cells treated with AS 100 nM and IPI 100 nM increased levels of phosphorylated eIF2α (**Figure 16a and 16d**), while all compounds were able to reduce levels of phosphorylated S6RP (**Figure 16a and 16e**). In Jurkat cells only AS 100 nM and IPI 100 nM increased p62 levels, while DOX and both inhibitors at 300 nM and 1000 nM reduced p62 (**Figure 16b and 16i**). Similar results were found for LC3B expression (**Figure16b and 16h**) Only Jurkat cells treated with DOX presented with cleaved PARP-1 bands, with a ratio between cleaved PARP-1 and PARP-1 of 2.50 (**Figure 16a**).

Figure 16 - Analysis by Western Blotting of biomarkers related to apoptosis, endoplasmic reticulum stress and autophagy in K562 and Jurkat cells treated with AS-605240 and IPI-145.

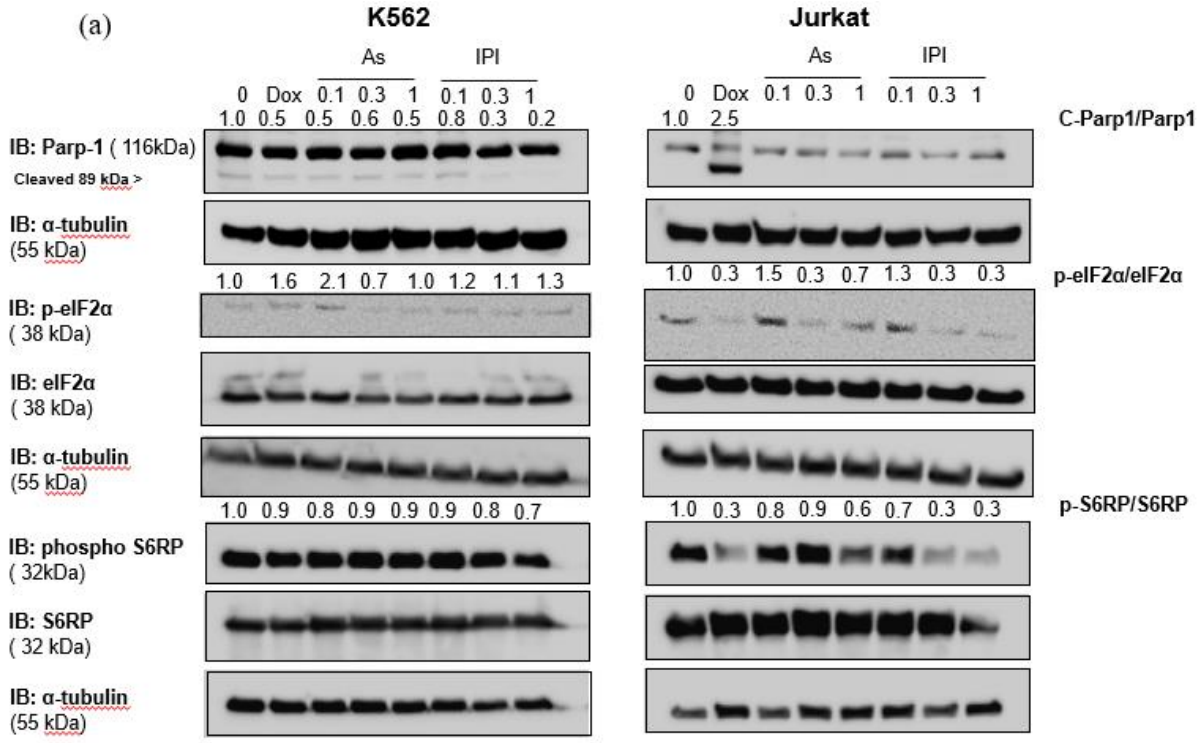

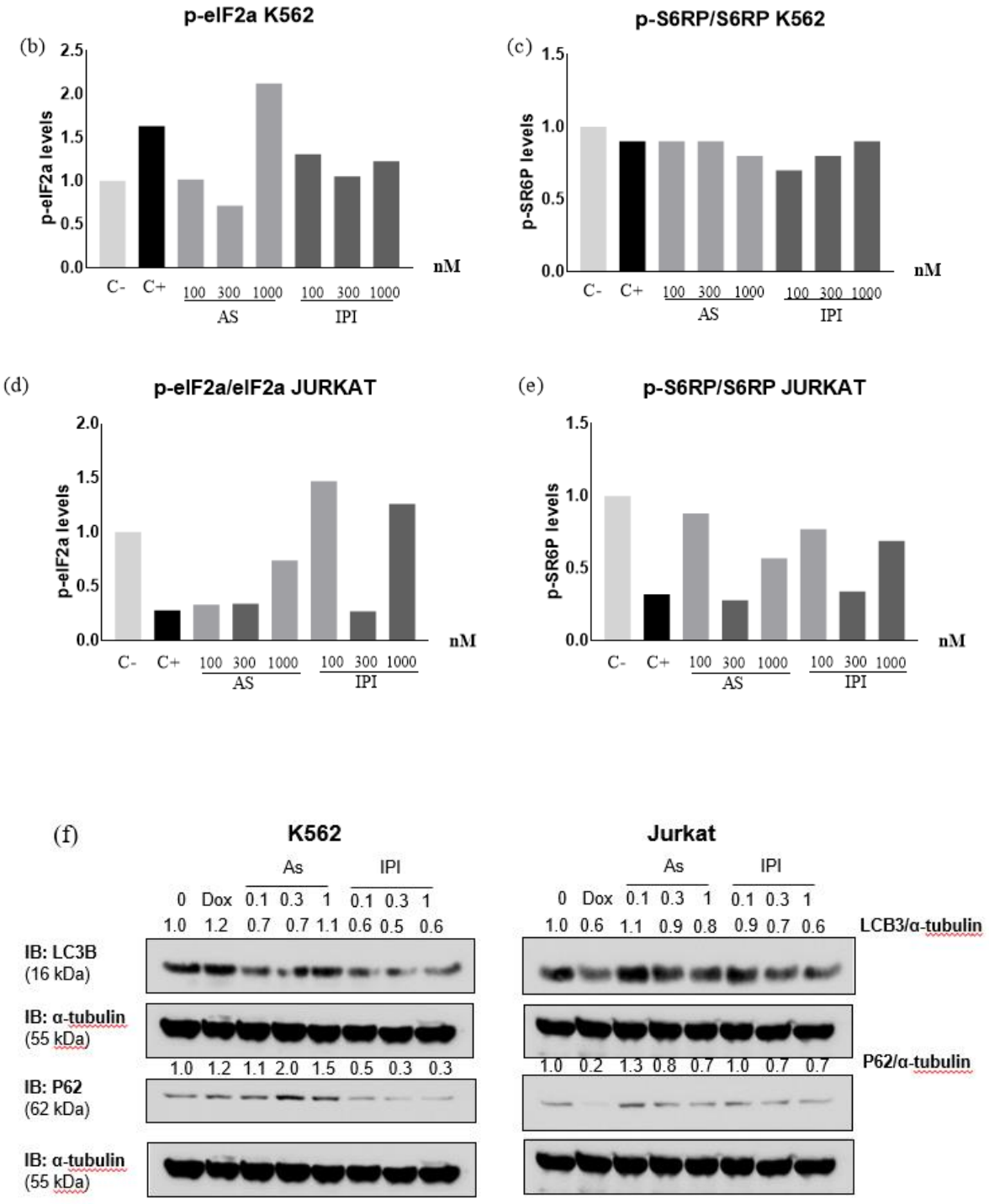
(b)
p-eIF2a K562
p-eIF2a levels
2.5
2.0
1.5
1.0
0.5
0.0
C- C+ 100 300 1000 100 300 1000
AS IPI
nM
(c)
p-S6RP/S6RP K562
p-SR6P levels
1.5
1.0
0.5
0.0
C- C+ 100 300 1000 100 300 1000
AS IPI
nM
(d)
p-eIF2a/eIF2a JURKAT
p-eIF2a levels
2.0
1.5
1.0
0.5
0.0
C- C+ 100 300 1000 100 300 1000
AS IPI
nM
(e)
p-S6RP/S6RP JURKAT
p-SR6P levels
1.5
1.0
0.5
0.0
C- C+ 100 300 1000 100 300 1000
AS IPI
nM
(f)
K562
As IPI
0 Dox 0.1 0.3 1 0.1 0.3 1
1.0 1.2 0.7 0.7 1.1 0.6 0.5 0.6
IB: LC3B
(16 kDa)
IB: α-tubulin
(55 kDa)
1.0 1.2 1.1 2.0 1.5 0.5 0.3 0.3
IB: P62
(62 kDa)
IB: α-tubulin
(55 kDa)
Jurkat
As IPI
0 Dox 0.1 0.3 1 0.1 0.3 1
1.0 0.6 1.1 0.9 0.8 0.9 0.7 0.6
LCB3/α-tubulin
1.0 0.2 1.3 0.8 0.7 1.0 0.7 0.7
P62/α-tubulin

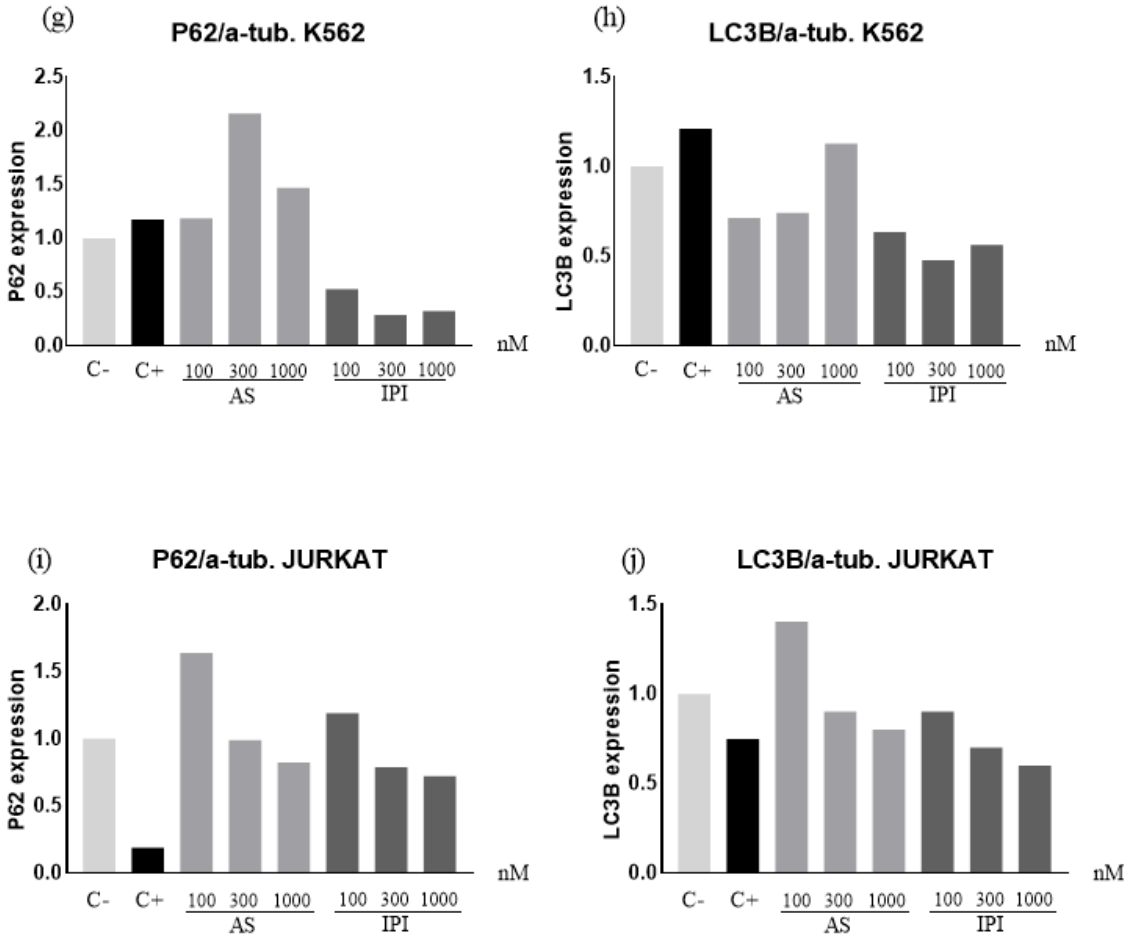

Source: Obtained from Dr. Anali Garnique and Prof Dr João Machado-Neto. Graphs made by the author.

Band quantification for Parp-1, eIF2α and S6RP for both cells (a). Antibodies used are indicated in the figure. Membranes were incubated with antibody for α-tubulin detection for control. N= 1. Phosphorylated eIF2α (b) and S6RP (c) alterations for K562 cells are shown. For Jurkat cells, phosphorylated eIF2α (d) and S6RP (e) alterations are also shown. Normalized band values for p62 and LC3B are displayed (f), along with p62 (g) and LC3B (h) graphs for K562 cells, and p62 (i) and LC3B (j) graphs for Jurkat cells.

6. DISCUSSION

The current study was performed to assess the potential of the PI3Kγ inhibitors AS-605240 and IPI-145 (duvelisib) to induce immunogenic cell death (ICD) *in vitro*. Both inhibitors showed antiproliferative effect in K562 cells, a CML cell line. Immunogenic cell death biomarkers were investigated, and CALR exposure was observed, as well as phosphorylation of eIF2α, the pathognomic factor for ICD. Additionally, markers of ER stress and autophagy were also assessed.

ICD is a type of regulated cell death first described by Casares in 2005 (Casares *et al*., 2005) as an event elicited by anthracyclines. ICD induction is of great interest in the perspective of anticancer treatment since it can activate immune response against the dying cells (Casares *et al*., 2005). This induction can be initiated by different stresses and produces antitumor immunity by the exposure or liberation of DAMPs such as CALR, HMGB1, ATP, HSPs, among others (Zhu; Mengqin *et al*., 2021).

Hematological malignancies are amongst the most common types of cancers globally, with the incidence increasing since 1990 (Zhang *et al*., 2023). Chronic myeloid leukemia accounts for about 15% of newly diagnosed leukemia. Before the development of TKI imatinib, annual mortality was about 10-20%. This targeted therapy altered the course of disease progression causing an improvement in 10-year survival rate to about 80-90% (Jabbour; Kantarjian, 2022). Tyrosine kinase inhibitors target the product of the fusion *Bcr-Abl1* and have revolutionized the treatment of CML. Due to CML being a chronic form of leukemia, most patients must remain in treatment indefinitely with possible adverse effects being monitored (Kronick *et al*., 2023). In addition to hematological side effects such as white and red blood cells alterations, some patients exhibit resistance, which occurs by mechanisms like *BCR-ABL1* mutations and overexpression, abnormal activity of drug transporters, among others (Alves *et al*., 2021). One of the strategies to overcome resistance is to target downstream of the product of the gene fusion or to target other relevant signaling pathways such as the PI3K/Akt/mTOR. In Imatinib, Nilotinib, and Ponatinib-resistant CML cells, BEZ235 (inhibitor of PI3K/mTOR) had antiproliferative activity (Singh *et al*., 2021). Furthermore, PI3K inhibition was capable of sensitizing CML progenitors and stem cells to Nilotinib (Airiau *et al*., 2013).

PI3K inhibition is a pharmacological strategy used for treatment of several types of neoplasms, as activation of the pathway occurs in 30-50% of human cancers (Martini *et al*., 2014) and results in resistance. AS-605240 is a specific PI3Kγ inhibitor and IPI-145 is a dual inhibitor of PI3Kγ/*δ* isoforms.

For the development of new therapies studies of pharmacokinetics are crucial to establish absorption, distribution, metabolism, and excretion parameters. SwissADME results indicate the molecules possess high gastrointestinal absorption, which along with water solubility is favorable for oral administration (Azman *et* al., 2022). Water solubility is also critical for handling and formulation of a molecule, constituting a very important parameter for parenteral administration as well. CYP interaction is another key aspect of drug development in view of their role in metabolic biotransformation, with 50-90% of molecules being substrates to the five principal isoforms CYP1A2, CYP2C19, CYP2C9, CYP2D6 and CYP3A4. Inhibition of CYPs is correlated to pharmacokinetics-related drug-drug interactions which can lead to toxicity and accumulation of drug metabolites. IPI-145 is a possible inhibitor of 3 of the 5 major CYPs, a fact that could lead to an increased toxicity as drug metabolites accumulate. AS-605240 is a probable inhibitor only of CYP1A2. Drug-likeness is a prediction based on several parameters for assessing the capability of a drug to be administered orally. This section of the SwissADME tool is based on five different rule sets for the parameter. The multiple estimates allow for a more comprehensive profile of the molecule tested. The pair of compounds tested passed all five drug-likeness rule sets, suggesting oral administration is favorable.

Target fishing for AS-605240 predicted Tyrosyl-DNA Phosphodiesterase 1 (Tdp1) and Serine/threonine-protein kinase haspin as possible off-targets of the inhibitor. Tdp1 is an enzyme involved in the repair of irreversible topoisomerase I-DNA complexes (Dexheimer *et al.*, 2008) and is a target for anticancer therapy. Haspin kinase is a protein involved in cell cycle control and mitosis (Liu *et al.*, 2023), being found over regulated in many cancer types. An anticorrelation with haspin expression and patient survival was found (Quadri; Sertic; Muzi-Falconi, 2022).

For IPI-145, target fishing found Tyrosine-protein kinase FYN and Serine/threonine-protein kinase TNNI3K as probable off targets. FYN is a member of the oncogene family and is implicated in the control of cell growth. The Ras/PI3K/Akt pathway can account for FYN's overexpression in many cancer types (Yadav; Denning, 2011). TNNI3K is a therapeutic target for cardiac disease, with its variants associated with many heart conditions such as arrhythmias and cardiomyopathy (Pham; Muñoz-martín; Lodder, 2021). The PI3K/Akt pathway participates in the pathogenesis of many heart conditions by regulation size and survival of cardiomyocytes, angiogenic processes and inflammation (Ghafouri-Fard *et al.*, 2022).

Both inhibitors were tested in K562 cells, a lineage of CML which was chosen after assessment of PI3Kγ expression by flow cytometry. Their antiproliferative activity was

evaluated indirectly by the trypan exclusion dye method, which showed low to moderate reduction in the number of viable cells after a 24-hour exposition to the inhibitors at concentrations ranging from 30 nM to 3000 nM. After detecting the presence of non-viable cells at 300, 1000 and 3000 nM, the two lowest concentrations were chosen for the subsequent flow cytometry experiments in a way to minimize off-target binding. Adverse side effects are a major concern for PI3K inhibitors, with the approved molecules of this type facing scrutiny as a consequence. PI3Kγ constitutes an interesting target due to enriched expression in leukocytes, which could possibly reduce off-target interactions and adverse effects (Drew *et al*., 2020). The low to moderate toxicity can constitute an interesting mechanism for a less aggressive approach to immunotherapy.

Besides the trypan exclusion assay, the cytostatic activity was also observed in the colony formation assay, in which the inhibitors were tested on K562 and Jurkat cells. Through this assay it was possible to notice a reduction in the number of K562 colonies for the AS-605240 at 1000 and 2000 nM, and for IPI-145 at 300, 1000 and 2000 nM. For Jurkat cells, the reduction of colonies was observed only at the highest concentration tested, suggesting at 2000 nM there are already off-target effects of the inhibitors, since PI3Kγ expression was not observed in this cell line. Those results are compatible with the levels of toxicity presented by the inhibitors previously and the colony reduction was attributed to a cytostatic effect. PI3K inhibition *in vitro* is found to be mostly cytostatic, which is likely due to the PI3K signaling roles as growth factor and its nutrient sensing activation (Okkenhaug; Graupera; Vanhaesebroeck, 2016). Commonly, cells that suffer inhibition of the PI3K pathway enter a nutrient deprived state, which is paired with the cellular stress alterations presented in this work. Also, PI3Kγ over-activation is associated with an oncogenic phenotype, promoting tumor cell proliferation (Dituri *et al*., 2012). In that manner, the inhibition of colony proliferation could indicate the target is being modulated by the compounds tested.

After observing reduction in viable cells and a cytostatic effect, flow cytometry experiments were conducted to assess possible cell morphology alterations induced by the molecules tested. For this end, K562 cells were exposed to AS-605240 and IPI-145 at 300 and 1000 nM for 24 hours. This period was chosen after verifying at this interval it was already possible to observe cell stress. Both compounds were able to induce morphology changes such as increase in the percentage of shrinkage and high granularity cells. Positive control DOX was also able to induce those changes. These morphological alterations reflect cell stress and are important indications of loss of viability. Loss of membrane integrity was observed only for IPI-145 at 1000 nM in the same experimental conditions. Those morphological aspects are

important to suggest that after contact with the inhibitors, cells are under significant stress conditions. Since the important DAMPs to evaluate ICD induction are liberated by cells in the process of dying, time of incubation is crucial for the detection of these biomarkers.

Going forward, the main goal was to evaluate the involvement of DAMPs and alterations correlated with ICD. Initially, the externalization of CALR was observed. CALR is exposed on the cell membrane earlier during ICD, even before apoptosis markers like the exposure of phosphatidylserine. CALR acts as a 'eat-me' phagocytic signal to antigen-presenting cells and is a crucial event in ICD, as it starts the immunogenic process (Kepp *et al*., 2014) by facilitating recognition of stressed and dying cells. Results obtained showed significant increase of CALR exposure for the experimental groups when compared to negative control and are an important indicator of the inhibitor's ability to induce immunogenic activation. Western blot results showed an increase in phosphorylated eIF2α was observed after incubation with AS-605240 at 100 nM and all concentrations tested of IPI-145 in K562 cells. For Jurkat cells, only AS-605240 and IPI-145 at 100 nM were able to increase levels of p-eIF2α. The phosphorylation of eIF2α is a crucial part of the ER stress response and is also considered a pathognomonic factor for ICD. The involvement of ER stress in ICD needs to be correlated with autophagy, as those are the two major pre-mortem stress responses in the phenomenon (Bezu *et al.*, 2018).

Western blot results also exhibit that for K562 cells, IPI-145 was able to reduce expression of the protein Sequestosome 1 (p62/SQSTM1) receptor, a classical selective autophagy receptor with roles in the ubiquitin-proteasome system, cellular metabolism and apoptosis. For Jurkat cells, all treatments except AS-60520 and IPI-145 at 100 nM were able to reduce p62 levels. p62 has different context-dependent impacts and its turnover usually reflects proteostasis. The transcription of p62 is modulated through conserved autophagy and the lysosomal regulator transcription factor EB whose nuclear localization is modulated by mTORC1, which is a downstream target of the PI3K pathway. p62 is one of the principal markers of the autophagic flux, along with LC3B, and p62 accumulation is correlated with defective autophagy (Kumar; Mills; Lapierre, 2022). LC3B levels in K562 cells were reduced by AS-605240 at 100 and 300 nM, and IPI-145 at all concentrations tested. In Jurkat cells LC3B was reduced by DOX, AS-605240 300 and 1000 nM, and all tested concentrations of IPI-145.

Unexpectedly, exposure to AS-605240 and IPI-145 increased the MFI of HMGB1 when compared to negative control, which differs from the HMGB1 liberation that was expected as a crucial ICD event. HMGB1 is responsible for mediation of pro-inflammatory

responses through TLR4 to stimulate processing and cross-presenting of the antigens presented by dying cells (Ahmed; Tait, 2020). This HMGB1-dependent activation of TLR4 is crucial to ICD immunogenicity although is not sufficient as a sign of its occurrence (Fucikova *et al*., 2020). Nuclear HMGB1 is extensively bound to DNA and associated with transcriptional regulation, DNA's repair and replicative machinery, telomere maintenance and nucleosome assembly (Ugrinova; Pasheva, 2017). Cytoplasmic HMGB1 is involved in immune responses such as increasing autophagy, inhibiting apoptosis and regulating mitochondrial function. Deregulation of HMGB1 is associated with many diseases, such as inflammatory disorders and cancer (Wang; Zhang, 2020). In cancer it appears that HMGB1 can exhibit paradoxical roles. For instance, nuclear and cytoplasmic HMGB1 increase autophagy and inhibit apoptosis in a manner that increases chemotherapy resistance. Concomitantly, nucleus HMGB1 promotes genomic stability (Wang; Zhang, 2020). One of the off-targets predicted for AS-605240, the Tdp1 protein, has major roles in DNA repair. It has been found that both Tdp1 and HMGB1 have protein-protein interactions with DNA polymerase β in the process of mammalian base excision repair (Prasad *et al.*, 2012).

Additionally, in the context of acute lung injury it has been found that the downstream pathways of HMGB1 in the plasma may lead to neutrophil infiltration, inflammatory cytokine release. HMGB1 binds to TLR-2 and TRL-4, which mediates inflammatory molecules such as TNF-α, IL-1β, IL-18, and IL-6. HMGB1 also activates an inflammatory response by activating the PI3K/AKT/mTOR pathway (Li *et al.*, 2020). In cells of acute myeloid leukemia, HMGB1 is found overexpressed, contributing to AML progression by inhibiting apoptosis, aiding in proliferation, and blocking myeloid differentiation. High expression of HMGB1 is correlated with the progression of lymphocytic leukemia and CML. HMGB1 is capable of inducing autophagy through PI3K-MEK-ERK and PI3K/Akt/mTORC1 pathways, mediating chemotherapy resistance in leukemia cells (Liu *et al.*, 2021).

These important DAMPs can be assessed *in vitro* and correlate with predicted ICD induction. In the context of colorectal cancer, it has been found that a combination of niparib (a PARP inhibitor) and a PI3K inhibitor (HS-173) was able to induce ICD in vitro and in vivo (Landry et al., 2020). PI3Kγ inhibition is an important strategy in the treatment of head and neck squamous carcinomas, with associated studies showing that in a cohort of patients, 30.5% contained mutations in the PI3K-Akt-mTOR pathway mostly in Pik3ca, Pik3cg, and Pten. A selective p110γ inhibitor, IPI-549, has shown some success when combined with other therapies. PI3Kγ inhibition of a murine model of head and neck squamous carcinoma present potent immunomodulatory and cytotoxic effects in poorly immunogenic tumors (Anderson et

al., 2021). To successfully assess if ICD is being induced by the inhibitors tested in the present work, more biomarkers need to be evaluated, such as heat-shock proteins, exposure of ERp57 and extracellular ATP.

In K562 and Jurkat cells, treatment with both inhibitors decreased levels of phosphorylated S6RP, a downstream target of the PI3K/AKT/mTOR pathway, with Jurkat cells exhibiting a more pronounced reduction. Jurkat cells were found to be PTEN-deficient and hyperresponsive to T-Cell receptor stimulation (Shan *et al*., 2000), which causes aberrant PI3K signaling (Gioia *et al.*, 2018). It has been found that isoform-selective class I inhibitors allow compensation from other isoforms (Okkenhaug; Graupera; Vanhaesebroeck, 2016). Additionally, kinase drug selectivity is a major pharmacological challenge due to the similarity of kinase drug pockets. Off-target effects are not uncommon and are a significant cause of toxicity (Zhang *et al.*, 2023). In that manner, even though Jurkat cells were not found to express PI3Kγ, they are a more susceptible target for PI3K inhibition, due to the active aberrant signaling. Likely, the inhibition of p-S6RP is due to inhibitors off-target binding to the available isoforms. K562 cells possess the BCR/ABL fusion gene which results in a TK which constitutively hyperactivates many signaling pathways including JAK/STAT and PI3K/Akt/mTOR pathways (Al-Rawashde *et al.*, 2022). Even though PI3Kγ is activated mostly through GPCRs (Nürnberg; Beer-Hammer, 2019) it has been reported that the BCR/ABL gene also increases p110γ expression (Hickey; Cotter, 2006). Since in CML all PI3K isoforms are aberrantly activated, it is possible that PI3Kγ inhibition is being compensated by the other isoforms (Okkenhaug; Graupera; Vanhaesebroeck, 2016).

Aberrant signaling, compensation from other isoforms and challenging kinase selectivity are some strategic challenges faced by PI3K inhibitors. The pathway remains an interesting target for pharmacological intervention, even though there are hurdles for development. One factor in favor of PI3K inhibition is the correlation between the pathway's activation and the occurrence of resistance against various anticancer agents (Okkenhaug; Graupera; Vanhaesebroeck, 2016), which favors combination therapy strategies. There is also increasing evidence for synergy between immunotherapeutic agents and chemotherapy (Pfirschke *et al.*, 2016). Combination strategies are also relevant for ICD induction, which contributes to address drug resistance (Zhai *et al.*, 2023).

In leukemia, one of the first lines of treatment is daunorubicin, an anthracycline and ICD inducer used to treat acute myeloid leukemia patients. With the current clinical protocols, about 70% of AML patients reach complete remission (Ocadlikova *et al.*, 2020). Even though treatment is established, the probability of relapse is high. There are also several described

resistance mechanisms associated with daunorubicin in AML cells, such as increased expression of drug efflux transporters, decreased activity of DNA topoisomerase II, and resistance through the apoptotic pathway. Gene mutations, namely FMS-like tyrosine kinase (FLT3) gene, are also responsible for chemotherapy resistance. The FLT3 mutation affects several kinase pathways, for instance PI3K/Akt/mTOR (Arwanih *et al.*, 2022). Daunorubicin was also found to increase PI3K activity and activate AKT, a downstream effector of the PI3K pathway. The PI3K/Akt pathway is involved in cell survival and PI3K signaling could contribute to daunorubicin resistance (Plo *et al.*, 1999). In light of the possible involvement of the PI3K pathway in, an interesting combination strategy could be associating daunorubicin and a PI3Kγ inhibitor in AML cells. Beyond that, selective PI3Kγ inhibitors could be an interesting strategy due to less inhibition of other PI3K isoforms and the capability to induce immunogenicity, which needs to be better evaluated.

7. CONCLUSION

PI3Kγ inhibitors AS-605240 and IPI-145 showed antiproliferative effects against K562 cells, while inducing cell stress and activating biomarkers correlated with ICD. In K562, the cell lineage expressing PI3Kγ, both inhibitors were able to increase cellular stress phenotypes such as high granularity and shrinkage. CALR exposure and p-eIF2$\boldsymbol{\alpha}$, markers of ER stress and immunogenicity were also induced by the inhibitors. In K562 cells, IPI-145 reduced expression of p62, which is correlated to effective autophagic flux. In that manner, it is likely that the PI3Kγ inhibitors tested were able to increase immunogenicity of susceptible cell lines. Further experiments are required to confirm these findings, such as repeating western blot experiments and evaluating other relevant biomarkers to confirm. Additionally, abnormal PI3K signaling could be correlated to drug resistance in an anticancer context. Thus, combination therapies with PI3K inhibitors constitute an interesting strategy to overcome resistance.

8. REFERENCES

AHMED, Asma; TAIT, Stephen W.G. Targeting immunogenic cell death in cancer. **Molecular Oncology** v. 14, n. 12, p. 2994–3006, 2020.

AIRIAU, K. *et al.* PI3K/mTOR pathway inhibitors sensitize chronic myeloid leukemia stem cells to nilotinib and restore the response of progenitors to nilotinib in the presence of stem cell factor. **Cell Death & Disease 2013 4:10** v. 4, n. 10, p. e827–e827, 2013.

ALLURI, Ramesh *et al*. Phosphoinositide 3-kinase inhibitor AS605240 ameliorates streptozotocin-induced Alzheimer 's disease like sporadic dementia in experimental rats. **EXCLI Journal** v. 19, p. 71, 2020.

AL-RAWASHDE, Futoon Abedrabbu *et al.* Thymoquinone Inhibits JAK/STAT and PI3K/Akt/ mTOR Signaling Pathways in MV4-11 and K562 Myeloid Leukemia Cells. **Pharmaceuticals 2022, Vol. 15, Page 1123**, [*s. l.*], v. 15, n. 9, p. 1123, 2022.

ALVES, Raquel *et al.* Resistance to Tyrosine Kinase Inhibitors in Chronic Myeloid Leukemia—From Molecular Mechanisms to Clinical Relevance. **Cancers** v. 13, n. 19, p. 4820 , 1 out. 2021.

ANDERSON, Kelvin *et al.* Inhibition of PI3K Isoform p110γ Increases Both Anti-Tumor and Immunosuppressive Responses to Aggressive Murine Head and Neck Squamous Cell Carcinoma with Low Immunogenicity. **Cancers**, [*s. l.*], v. 13, n. 5, p. 1–17, 2021.

ANDRÉ, Fabrice *et al*. Alpelisib for PIK3CA-Mutated, Hormone Receptor–Positive Advanced Breast Cancer. **New England Journal of Medicine** v. 380, n. 20, p. 1929–1940, 2019.

ARWANIH, Elly Y *et al.* Resistance Mechanism of Acute Myeloid Leukemia Cells Against Daunorubicin and Cytarabine: A Literature Review. **Cureus**, [*s. l.*], v. 14, n. 12, 2022. Disponível em: /pmc/articles/PMC9885730/

AZMAN, Maisarah *et al*. Intestinal Absorption Study: Challenges and Absorption Enhancement Strategies in Improving Oral Drug Delivery. Pharmaceuticals v. 15, n. 8 , 1 ago. 2022. Disponível em: </pmc/articles/PMC9412385/>. Acesso em: 29 nov. 2023.

BAEKER BISPO, Jordan A.; PINHEIRO, Paulo S.; KOBETZ, Erin K. Epidemiology and Etiology of Leukemia and Lymphoma. **Cold Spring Harbor Perspectives in Medicine**, [*s. l.*], v. 10, n. 6, 2020.

BAGHBAN, Roghayyeh *et al*. Tumor microenvironment complexity and therapeutic implications at a glance. **Cell Communication and Signaling 2020** 18:1 v. 18, n. 1, p. 1–19, 2020.

BEZU, Lucillia *et al*. eIF2α phosphorylation is pathognomonic for immunogenic cell death. **Cell Death and Differentiation** v. 25, n. 8, p. 1375, 2018.

CASARES, Noelia *et al*. Caspase-dependent immunogenicity of doxorubicin-induced tumor cell death. **The Journal of Experimental Medicine** v. 202, n. 12, p. 1691, 2005.

CHANG, Jun *et al*. Targeting PIK3CG in combination with paclitaxel as a potential therapeutic regimen in claudin-low breast cancer. **Cancer Management and Research** v. 12, p. 2641–2651, 2020.

CHEAH, Chan Yoon; FOWLER, Nathan H. Idelalisib in the management of lymphoma. **Blood** v. 128, n. 3, p. 331–336, 2016.

CHEN, Lezong *et al*. Changing causes of death in persons with haematological cancers 1975–2016. **Leukemia 2022** 36:7 v. 36, n. 7, p. 1850–1860, 2022.

Chronic Myeloid Leukemia (CML) | Penn Medicine. Available at: <https://www.pennmedicine.org/cancer/types-of-cancer/leukemia/types-of-leukemia/chronic-myeloid-leukemia>.

DAINA, Antoine; MICHIELIN, Olivier; ZOETE, Vincent. SwissADME: a free web tool to evaluate pharmacokinetics, drug-likeness and medicinal chemistry friendliness of small molecules. **Scientific Reports 2017 7:1** v. 7, n. 1, p. 1–13, 2017.

DAMLAJ, Moussab; EL FAKIH, Riad; HASHMI, Shahrukh K. Evolution of survivorship in lymphoma, myeloma and leukemia: Metamorphosis of the field into long term follow-up care. **Blood Reviews** v. 33, p. 63–73, 2019.

DEININGER, M. W.N.; GOLDMAN, J. M.; MELO, J. V. The molecular biology of chronic myeloid leukemia. **Blood**, [*s. l.*], v. 96, n. 10, p. 3343–3356, 2000.

DE SANTIS, Maria Chiara *et al*. Targeting PI3K signaling in cancer: Challenges and advances. **Biochimica et Biophysica Acta (BBA) -** Reviews on Cancer v. 1871, n. 2, p. 361–366, 2019.

DE VERA, Albert A. *et al*. Immuno-oncology agent IPI-549 is a modulator of P-glycoprotein (P-gp, MDR1, ABCB1)-mediated multidrug resistance (MDR) in cancer: in vitro and in vivo. **Cancer letters** v. 442, p. 91, 2019.

DEXHEIMER, Thomas S. *et al.* Tyrosyl-DNA Phosphodiesterase as a Target for Anticancer Therapy. **Anti-cancer agents in medicinal chemistry**, [*s. l.*], v. 8, n. 4, p. 381, 2008. Disponível em: /pmc/articles/PMC2443942/.

DITURI, Francesco *et al.* PI3K class IB controls the cell cycle checkpoint promoting cell proliferation in hepatocellular carcinoma. **International Journal of Cancer** v. 130, n. 11, p. 2505–2513, 2012.

DREW, Samuel L. *et al.* Discovery of Potent and Selective PI3Kγ Inhibitors. **Journal of Medicinal Chemistry** v. 63, n. 19, p. 11235–11257, 2020.

DREYLING, Martin *et al*. Phase II study of copanlisib, a PI3K inhibitor, in relapsed or refractory, indolent or aggressive lymphoma. **Annals of Oncology** v. 28, n. 9, p. 2169–2178, 2017.

FADERL, Stefan *et al*. The Biology of Chronic Myeloid Leukemia. https://doi.org/10.1056/NEJM199907153410306 v. 341, n. 3, p. 164–172, 1999.

FALASCA, Marco; MAFFUCCI, Tania. Targeting p110gamma in gastrointestinal cancers: Attack on multiple fronts. **Frontiers in Physiology** v. 5, n. OCT, p. 116069, 15 oct. 2014.

FDA Briefing Document Oncologic Drugs Advisory Committee Meeting Phosphatidylinositol 3-Kinase (PI3K) Inhibitors in Hematologic Malignancies, 2022.

FDA to close the door on single-arm approvals to PI3K blood cancer drugs. Available at: <https://www.fiercepharma.com/pharma/citing-unprecedented-safety-signals-fda-plots-closing-door-single-arm-approvals-pi3k-blood>.

FUCIKOVA, Jitka *et al.* Detection of immunogenic cell death and its relevance for cancer therapy. **Cell Death & Disease 2020** 11:11 v. 11, n. 11, p. 1–13, 2020.

GALLUZZI, Lorenzo *et al*. Classification of current anticancer immunotherapies. **Oncotarget** v. 5, n. 24, p. 12472, 2014.

GALLUZZI, Lorenzo *et al.* Consensus guidelines for the definition, detection and interpretation of immunogenic cell death. **Journal for Immunotherapy of Cancer** v. 8, n. 1, p. 70, 2020.

GARG, Abhishek D. *et al*. Immunogenic cell death. The International Journal of **Developmental Biology** v. 59, n. 1-2–3, p. 131–140, 2015.

GHAFOURI-FARD, Soudeh *et al.* Interplay between PI3K/AKT pathway and heart disorders. **Molecular Biology Reports**, [*s. l.*], v. 49, n. 10, p. 9767–9781, 2022.

GIOIA, Louis *et al.* A genome-wide survey of mutations in the Jurkat cell line. **BMC Genomics**, [*s. l.*], v. 19, n. 1, p. 1–13, 2018.

GU, Dong yan *et al*. Development of PI3Kγ selective inhibitors: the strategies and application. **Acta Pharmacologica Sinica** 2023 p. 1–10, 2023.

HAMADA, S.; FUJITA, S. DAPI staining improved for quantitative cytofluorometry. **Histochemistry** v. 79, n. 2, p. 219–226, 1983.

HANAHAN, Douglas. Hallmarks of Cancer: New Dimensions. Cancer Discovery v. 12, n. 1, p. 31–46, 2022.

HICKEY, Fionnuala B.; COTTER, Thomas G. BCR-ABL Regulates Phosphatidylinositol 3-Kinase-p110γ Transcription and Activation and Is Required for Proliferation and Drug Resistance. **Journal of Biological Chemistry**, [*s. l.*], v. 281, n. 5, p. 2441–2450, 2006.

JABBOUR, Elias; KANTARJIAN, Hagop. Chronic myeloid leukemia: 2022 update on diagnosis, therapy, and monitoring. **American Journal of Hematology** v. 97, n. 9, p. 1236–1256, 2022.

KEYKHAEI, Mohammad *et al*. A global, regional, and national survey on burden and Quality of Care Index (QCI) of hematologic malignancies; global burden of disease systematic analysis 1990–2017. **Experimental Hematology and Oncology** v. 10, n. 1, p. 1–15, 2021.

KROEMER, Guido *et al.* Immunogenic cell stress and death. **Nature Immunology 2022 23:4**, [*s. l.*], v. 23, n. 4, p. 487–500, 2022.

KRONICK, Olivia *et al.* Hematological Adverse Events with Tyrosine Kinase Inhibitors for Chronic Myeloid Leukemia: A Systematic Review with Meta-Analysis. **Cancers** v. 15, n. 17, 2023.

KRYSKO, Dmitri V. *et al.* Immunogenic cell death and DAMPs in cancer therapy. **Nature Reviews Cancer**. [S.l Nature Publishing Group, 2012.

KUMAR, Anita V.; MILLS, Joslyn; LAPIERRE, Louis R. Selective Autophagy Receptor p62/SQSTM1, a Pivotal Player in Stress and Aging. **Frontiers in Cell and Developmental Biology**, [*s. l.*], v. 10, p. 793328, 2022.

LADYGINA, Nadia *et al.* PI3Kγ kinase activity is required for optimal T-cell activation and differentiation. **European Journal of Immunology**, [*s. l.*], v. 43, n. 12, p. 3183–3196, 2013.

LANAHAN, Stephen M.WYMANN, Matthias P.; LUCAS, Carrie L. The role of PI3Kγ in the immune system: new insights and translational implications. **Nature Reviews Immunology 2022** 22:11 v. 22, n. 11, p. 687–700, 2022.

LANDRY, M. R. *et al.* Low dose novel PARP-PI3K inhibition via nanoformulation improves colorectal cancer immunoradiotherapy. **Materials Today Bio**, [*s. l.*], v. 8, p. 100082, 2020.

Leukemia - Symptoms and causes - Mayo Clinic. **Available at: https://www.mayoclinic.org/diseases-conditions/leukemia/symptoms-causes/syc-20374373.** Access on: November, 2023.

LEWIS, William D.; LILLY, Seth; JONES, Kristin L. Lymphoma: Diagnosis and Treatment. **American Family Physician**, [*s. l.*], v. 101, n. 1, p. 34–41, 2020.

LI, Ruiting *et al.* HMGB1/PI3K/Akt/mTOR Signaling Participates in the Pathological Process of Acute Lung Injury by Regulating the Maturation and Function of Dendritic Cells. **Frontiers in Immunology**, [*s. l.*], v. 11, p. 1104, 2020.

LIMA, Keli *et al.* Reversine exhibits antineoplastic activity in JAK2V617F-positive myeloproliferative neoplasms. **Scientific Reports 2019 9:1**, [*s. l.*], v. 9, n. 1, p. 1–9, 2019.

LIU, Lulu *et al.* HMGB1: an important regulator of myeloid differentiation and acute myeloid leukemia as well as a promising therapeutic target. **Journal of Molecular Medicine (Berlin, Germany)**, [*s. l.*], v. 99, n. 1, p. 107, 2021.

LIU, Yongjian *et al.* Function and inhibition of Haspin kinase: targeting multiple cancer therapies by antimitosis. **The Journal of pharmacy and pharmacology**, [*s. l.*], v. 75, n. 4, p. 445–465, 2023.

MARTINI, Miriam *et al*. PI3K/AKT signaling pathway and cancer: an updated review. **Annals of Medicine** v. 46, n. 6, p. 372–383, 2014.

MCKINNON, Katherine M. Flow cytometry: An overview. **Current Protocols in Immunology** v. 2018, p. 5.1.1-5.1.11, 2018.

NOOROLYAI, Saeed *et al*. The relation between PI3K/AKT signalling pathway and cancer. **Gene** v. 698, p. 120–128, 2019.

NÜRNBERG, Bernd; BEER-HAMMER, Sandra. Function, Regulation and Biological Roles of PI3Kγ Variants. **Biomolecules** v. 9, n. 9, 2019.

OBEID, Michel *et al*. Calreticulin exposure dictates the immunogenicity of cancer cell death. **Nature Medicine 2006** 13:1 v. 13, n. 1, p. 54–61, 2006.

OCADLIKOVA, Darina *et al.* A Screening of Antineoplastic Drugs for Acute Myeloid Leukemia Reveals Contrasting Immunogenic Effects of Etoposide and Fludarabine. **International Journal of Molecular Sciences**, [*s. l.*], v. 21, n. 18, p. 1–20, 2020.

OKKENHAUG, Klaus; GRAUPERA, Mariona; VANHAESEBROECK, Bart. Targeting PI3K in cancer: impact on tumor cells, their protective stroma, angiogenesis and immunotherapy. **Cancer discovery**, [*s. l.*], v. 6, n. 10, p. 1090, 2016.

PAPA, Antonella; PANDOLFI, Pier Paolo. The PTEN–PI3K Axis in Cancer. **Biomolecules** v. 9, n. 4, 2019.

PÉREZ-JIMÉNEZ, Mario; DERÉNYI, Imre; SZÖLLŐSI, Gergely J. The structure of the hematopoietic system can explain chronic myeloid leukemia progression. **Scientific Reports 2023** 13:1 v. 13, n. 1, p. 1–12, 2023.

PFIRSCHKE, Christina *et al.* Immunogenic chemotherapy sensitizes tumors to checkpoint blockade therapy. **Immunity**, [*s. l.*], v. 44, n. 2, p. 343, 2016.

PHAM, Caroline; MUÑOZ-MARTÍN, Noelia; LODDER, Elisabeth M. The Diverse Roles of TNNI3K in Cardiac Disease and Potential for Treatment. **International Journal of Molecular Sciences**, [*s. l.*], v. 22, n. 12, 2021.

POPHALI, Priyanka A.; PATNAIK, Mrinal M. The Role of New Tyrosine Kinase Inhibitors in Chronic Myeloid Leukemia. **Cancer journal** (Sudbury, Mass.) v. 22, n. 1, p. 40, 2016.

PLO, I. *et al.* The phosphoinositide 3-kinase/Akt pathway is activated by daunorubicin in human acute myeloid leukemia cell lines. **FEBS Letters**, [*s. l.*], v. 452, n. 3, p. 150–154, 1999.

PRASAD, Rajendra *et al.* Pol β associated complex and base excision repair factors in mouse fibroblasts. **Nucleic Acids Research**, [*s. l.*], v. 40, n. 22, p. 11571–11582, 2012.

QUADRI, Roberto; SERTIC, Sarah; MUZI-FALCONI, Marco. Roles and regulation of Haspin kinase and its impact on carcinogenesis. **Cellular Signalling**, [*s. l.*], v. 93, p. 110303, 2022.

RASCIO, Federica *et al*. The Pathogenic Role of PI3K/AKT Pathway in Cancer Onset and Drug Resistance: An Updated Review. **Cancers** v. 13, n. 16, 2021.

RODRIGUEZ-ABREU, D; BORDONI, A; ZUCCA, E. Epidemiology of hematological malignancies. **Hematology for the Medical Oncologist** v. 18, p. i3–i8 , 2007.

RÜCKLE, Thomas; SCHWARZ, Matthias K., Rommel, Christian. PI3Kγ inhibition: towards an "aspirin of the 21st century?" **Nature Reviews Drug Discovery 2006** 5:11 v. 5, n. 11, p. 903–918, 2006.

SALA, Valentina *et al*. Roles of phosphatidylinositol 3 kinase gamma (PI3Kγ) in respiratory diseases. **Cell Stress** v. 5, n. 4, p. 40, 2021.

SAMUELS, Yardena; WALDMAN, Todd. Oncogenic Mutations of PIK3CA in Human Cancers. **Current topics in microbiology and immunology**. [S.l.]: NIH Public Access, 2010. 347 v. p. 21–41.

SHAN, Xiaochuan *et al.* Deficiency of PTEN in Jurkat T Cells Causes Constitutive Localization of Itk to the Plasma Membrane and Hyperresponsiveness to CD3 Stimulation. **Molecular and Cellular Biology**, [*s. l.*], v. 20, n. 18, p. 6945, 2000.

SHAYESTEH, Laleh *et al*. PIK3CA is implicated as an oncogene in ovarian cancer. **Nature Genetics 1999** 21:1 v. 21, n. 1, p. 99–102, 1999.

SINGH, Priyanka et al. Combating TKI resistance in CML by inhibiting the PI3K/Akt/mTOR pathway in combination with TKIs: a review. **Medical Oncology 2021** 38:1 v. 38, n. 1, p. 1–16, 2021.

STROBER, Warren. Trypan Blue Exclusion Test of Cell Viability. **Current protocols in immunology** v. 111, n. 1, p. A3.B.1, 2015.

TAKEDA, Andrew J. *et al.* Human PI3Kγ deficiency and its microbiota-dependent mouse model reveal immunodeficiency and tissue immunopathology. **Nature Communications** v. 10, n. 1, p. 1–12, 2019.

TANGUDU, Naveen Kumar *et al*. Duvelisib: A 2018 Novel FDA-Approved Small Molecule Inhibiting Phosphoinositide 3-Kinases. **Pharmaceuticals** v. 12, n. 2, 2019.

THIAN, Marini *et al*. Germline biallelic PIK3CG mutations in a multifaceted immunodeficiency with immune dysregulation. **Haematologica** v. 105, n. 10, 2020.

UGRINOVA, I.; PASHEVA, E. HMGB1 Protein: A Therapeutic Target Inside and Outside the Cell. **Advances in Protein Chemistry and Structural Biology**, [*s. l.*], v. 107, p. 37–76, 2017.

WANG, Shumin; ZHANG, Yi. HMGB1 in inflammation and cancer. **Journal of Hematology & Oncology**, [*s. l.*], v. 13, n. 1, 2020.

What Is Chronic Myeloid Leukemia? | Leukemia Types | American Cancer Society. Available at: <https://www.cancer.org/cancer/types/chronic-myeloid-leukemia/about/what-is-cml.html>.

YADAV, Vipin; DENNING, Mitchell F. Fyn is Induced by Ras/PI3K/Akt Signaling and is Required for Enhanced Invasion/Migration. **Molecular Carcinogenesis**, [*s. l.*], v. 50, n. 5, p. 346, 2011.

YANG, Jing *et al*. Targeting PI3K in cancer: Mechanisms and advances in clinical trials .Molecular Cancer. [S.l.]: **BioMed Central** Ltd, 2019.

YU, Miaomiao *et al*. Development and safety of PI3K inhibitors in cancer. **Archives of Toxicology** v. 97, n. 3, p. 635, 2023.

ZHAI, Jiaqi *et al.* Chemotherapeutic and targeted drugs-induced immunogenic cell death in cancer models and antitumor therapy: An update review. **Frontiers in Pharmacology**, [*s. l.*], v. 14, 2023.

ZHANG, Mingzhen *et al.* Strategy toward Kinase-Selective Drug Discovery. **Journal of Chemical Theory and Computation**, [*s. l.*], v. 19, n. 5, p. 1615–1628, 2023.

ZHANG, Nan *et al*. Global burden of hematologic malignancies and evolution patterns over the past 30 years. **Blood Cancer Journal** 2023 13:1 v. 13, n. 1, p. 1–13, 2023.

ZHOU, Linghui *et al.* Global, regional, and national burden of Hodgkin lymphoma from 1990 to 2017: Estimates from the 2017 Global Burden of Disease study. **Journal of Hematology and Oncology** v. 12, n. 1, p. 1–13, 2019.

ZHU, Jingyu *et al*. Discovery of a novel phosphoinositide 3-kinase gamma (PI3Kγ) inhibitor against hematologic malignancies and theoretical studies on its PI3Kγ-specific binding mechanisms. **RSC Advances** v. 9, n. 35, p. 20207–20215, 2019.

ZHU, Mengqin *et al.* Immunogenic Cell Death Induction by Ionizing Radiation. **Frontiers in Immunology** v. 12, p. 705361, 2021.